CONF-8609142--8

SUPERCOMPUTER COMPUTATIONS RESEARCH INSTITUTE

Florida State University

Tallahassee, FL 32306-4052

CONF-8609142--8

December 18, 1986

DE87 014139

FINITE SIZE SCALING AND LATTICE GAUGE THEORY[†]

by

Bernd A. Berg

FSU-SCRI-86-89

FG05-87ER40319

FC05-85ER25000

[†] Invited lecture given at "Lattice Gauge Theory 1986", Brookhaven National Laboratory, Upton, NY September, 1986.

FINITE SIZE SCALING AND LATTICE GAUGE THEORY

Bernd A. Berg

Department of Physics and
Supercomputer Computations Research Institute
The Florida State University
Tallahassee, Fl 32306, USA

ABSTRACT

Finite size (Fisher) scaling is investigated for four dimensional SU(2) and SU(3) lattice gauge theories without quarks. It allows to disentangle violations of (asymptotic) scaling and finite volume corrections. Mass spectrum, string tension, deconfinement temperature and lattice β-function are considered. For appropriate volumes, Monte Carlo investigations seem to be able to control the **finite volume** continuum limit. Contact is made with Lüscher's small volume expansion and possibly also with the asymptotic large volume behaviour.

1) INTRODUCTION

Pure lattice gauge theory is a regularization of non-abelian gauge theory. Our aim is to remove the regularization with Monte Carlo (MC) simulations as a computational tool. Primarily, the analysis of MC data should be based on first principles, like for instance, a positive definite transfer matrix, finite size scaling and asymptotic scaling. Secondly, heuristic information from strong coupling expansions, string theory, analogies with spin models etc. may be of value. However, emphasizing analogies can also be dangerous and may spoil an unbiased understanding of lattice gauge theories from first principles.
Finite size scaling concepts were introduced by Fisher [1]. For lattice gauge theory a detailed discussion will be given in Ref. [2]. Our concept is to analyze numerical data for physical quantities in terms of a scaling variable

$$z = \frac{L}{\xi}. \tag{1}$$

L is a length that is characteristic for the finite size of the system and ξ is a suitable correlation length. Examples are

$$z_0 = m(0^{++})L, \quad z_2 = m(2^{++})L \quad \text{and} \quad z_k = \sqrt{K}L. \tag{2a}$$

Here $m(0^{++})$ and $m(2^{++})$ are the mass gaps corresponding to the representations $A1^{++}$ and E^{++} of the cubic group, and K is a lattice string tension. We have assumed lattices of shape $L^3 L_z$ with $L_z \gg L$. For the deconfinement temperature most investigations are done on $L_t L^3$, $L_t \leq L$ lattices and the appropriate Fisher variable is

$$z_T = T_c L = \frac{L}{L_t}. \tag{2b}$$

Why should we bother to use Fisher variables to analyze our MC data? We will see that these variables provide a very convenient way to disentangle violations of (asymptotic) scaling and finite size problems. By simply plotting results in z-variables one may gain a lot of insight [3]. In view of data with finite statistics it is mainly a practical advantage, namely z-variables allow us to use all data together for studying finite size effects. This is not true for an approach where one tries to extract the infinite volume limit at each fixed β-value and then to approach the $\beta \to \infty$ limit. Again by reasons of practical nature, several z-variables should be used, because otherwise spurious statistical errors may become introduced into our analysis.

How does it work? Fisher's scaling limit is

$$M(z) = \lim_{\beta \to \infty} M(\beta, L)|_{z=\text{const}}. \tag{3}$$

Here $M(\beta, L)$ is supposed to be measured in units such that $M(z)$ and $M = lim_{z\to\infty} M(z)$ are well-defined. Let us outline the relevant features of the limit (3).
1) Assuming critical behaviour, equation (3) relates L and β at fixed z such that $L = L(\beta) \to \infty$ for $\beta \to \infty$. Neglecting (a/L)-corrections to Fisher scaling, the β-dependence is governed by scaling for mass ratios and by asymptotic scaling, if M is expressed in unit of Λ_L.
2) At each fixed z, limiting results ($\beta \to \infty$) are universal, i. e. independent of the particular regularization used. For instance, special cases are the lattice regularization and the $\overline{MS}$-scheme used in perturbative calculations. The infinite volume limit is approached as $z \to \infty$.
Both remarks are illustrated with Figure 1. Imagine MC data, for example for the mass gap in units of Λ_L. At large β, fixed z, the universal curve is approached. Corrections to Fisher scaling are of order a/L. For β large this is exponentially small in β and leading are the power law corrections $(\beta^{-1}, ...)$ to asymptotic scaling. Data at different z-values can only be used to discuss asymptotic scaling violations, if there is no or neglegible z-dependence along the universal curve. This would be the case, if the data are sufficiently close to the infinite volume limit. Normally such an assumption is just wrong.

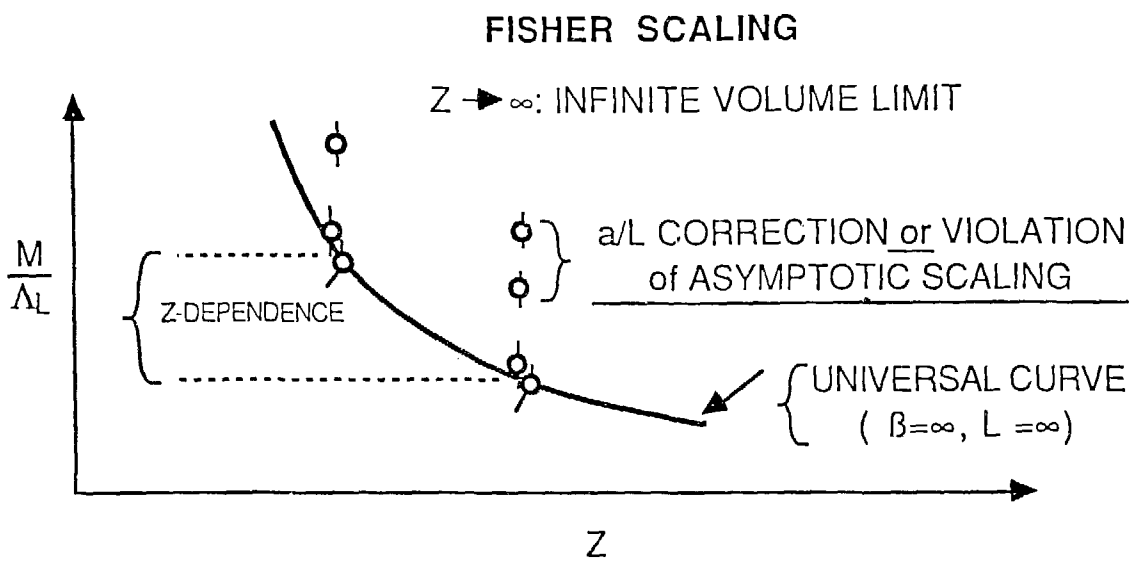

Figure 1 :

Illustration of Fisher scaling with hypothetical MC data.

MC data, on any lattice size (large or not), are always at finite z. The infinite lattice limit (3) is easier to control than the infinite volume continuum limit. The latter limit is the most difficult one of all! The fixed z limit (3) leads us to a continuous box of finite physical size. Lattice gauge theory in a continuous $l^3 l_z$-box box was first studied by 't Hooft [4] (we use lower case letters, $l^3 l_z$, for the size in physical units). Small volumes allow analytic (small z_0) calculations, pioneered by Lüscher [5]. Appropriate MC calculations on $L^3 L_z$-lattices ($L_z \gg L$) were begun by Billoire, Vohwinkel and the present author [6,7] (detailed results [2] are yet unpublished). Figure 2 is reproduced from Ref.[4] and exhibits an elongated continuous box. Let us take the transfer matrix in L_z-directions (a_3 in the figure). Expectation values of operators local in t_z-time read:

$$< \mathbf{O} > = \frac{\sum_n < n|\mathbf{O}|n > \ \mathbf{e}^{-\mathbf{E_n} l_z}}{\sum_n \mathbf{e}^{-\mathbf{E_n} l_z}}. \tag{4}$$

Clearly, l_z^{-1} plays the role of a temperature [4]. We will call

$$T_b = l_z^{-1} \tag{5}$$

box temperature to distinguish it from the physical temperature. Our strategy is now to study the physics of a continuous box. We begin with small z_0-values and proceed towards larger and larger z_0.

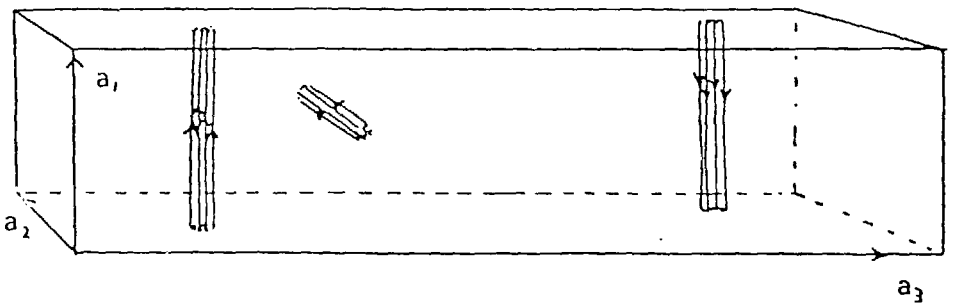

Figure 2 :

Elongated box at finite temperature. Strings may be produced by thermal oscillations [4].

1a) Very small z_0

Lüscher's small z_0-expansion is carried out for an $l^3\infty$-box. For $SU(N)$ there are N^3 gauge inequivalent classical vacuum configurations [4]. Following Gonzales-Arroyo, Jurkiewicz and Korthals-Altes [8], I will call these configurations *"torons"*. The perturbative small volume expansion is carried out in one fixed toron sector and an N^3-fold degeneracy is found [5] to hold to all orders.

Figure 3, from the study [9] of the two-dimensional $O(n)$ σ-model, depicts the original hope of the small volume expansion, namely a smooth and early crossover from the small volume z_0-behaviour to the constant infinite volume z_0-limit. Whereas the model is solved exactly for $n \to \infty$, numerical analysis is still needed for finite n. Even for these simple models, the numerical analysis by Bender et. al.[10] did not confirm a simple crossover behaviour for the interesting $O(3)$-case.
Small z_0-results for $SU(2)$ gauge theory are depicted in Figure 4a and 4b. Mass results in units of $\Lambda_{\overline{MS}}$ (Figure 4a) show an extremely rapid crossover from the small volume to the large volume behaviour. This has been made explicit by our MC simulation [6], and our conclusion is that $SU(2)$ MC simulations do not allow to match quantitavely accurate on small volume calculations for single masses. However, the $0^+/2^+$ mass ratio (Figure 4b) exhibits a very smooth behaviour with increasing z_0, and our MC results of Ref.[7] support this behaviour far beyond the range of convergence of the small z_0 expansion.

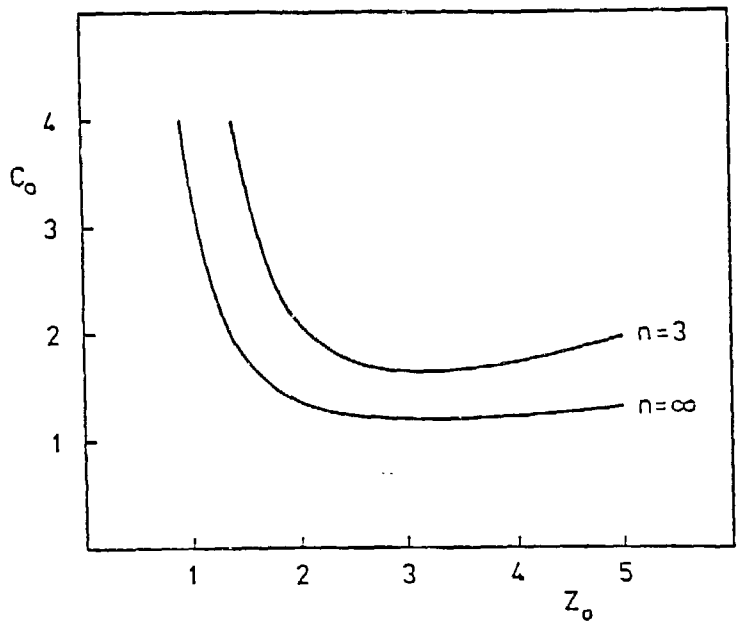

Figure 3 :

Lüscher's small volume expansion for the $O(n)$ σ-models [9]. Plot of $C_0(z_0) = m/\Lambda_{\overline{MS}}$ versus z_0 for $n = 3$ and $n = \infty$, keeping only the leading order. The curves for intermediate values of n are sandwiched between the $n = 3$ and $n = \infty$ curves.

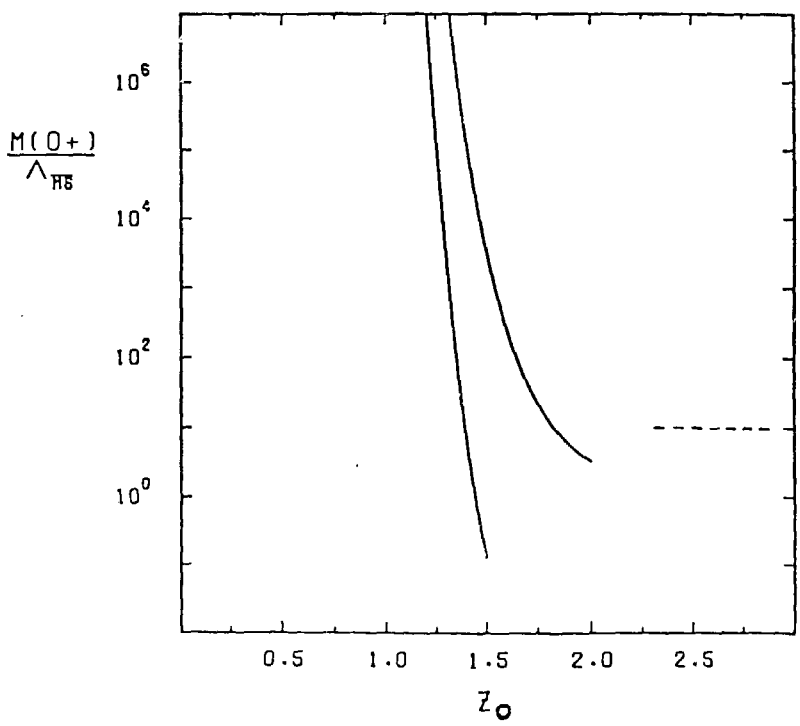

Figure 4a : (previous page)

$SU(2)$ energy gap $m(0^+)$ as a function of z_0 [5]. The two curves differ by the way the perturbative results are truncated. The dashed line indicates typical MC estimates of the infinite-volume mass gap.

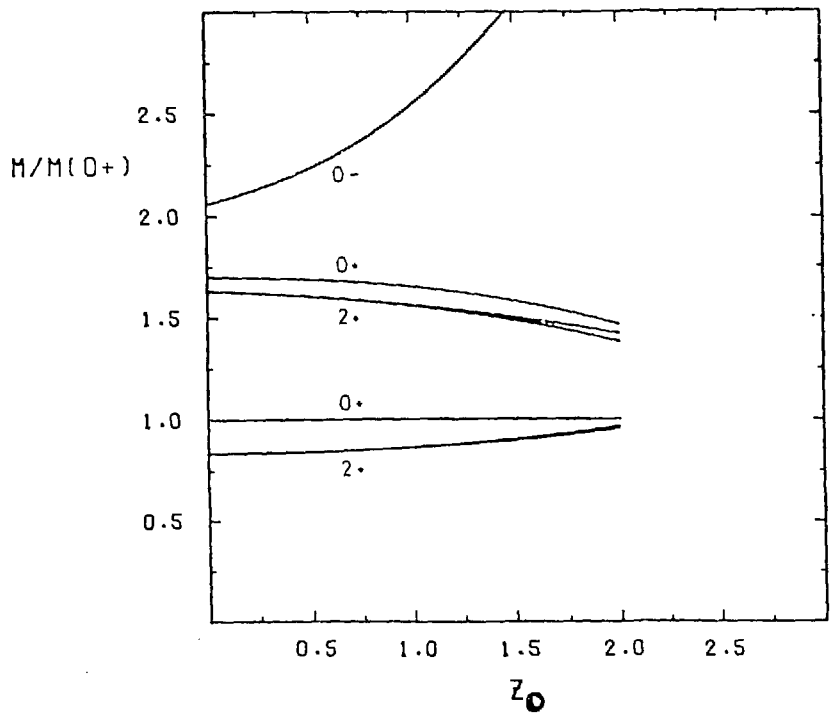

Figure 4b :

$SU(2)$ mass ratios as function of z_0 [5]. From Figure 4a it is indicated that the radius of convergence does not extend beyond $z_0 \approx 1.3$.

1b) Increasing z_0

Let us follow Ref.[4] and consider Figure 2. The Boltzmann factor of a string in a_1-direction is $\exp(-\beta K a_1)$, where K is 't Hooft's [4] definition of the string tension. On the lattice, we will call a loop of the type of Figure 2, that is closed by means of the

periodic boundary conditions, a Polyakov [11] loop. Using Polyakov loops, MC calculations of the string tension were first carried out by Parisi et. al.[12]; see Ref.[13] for $SU(2)$. At finite β, on the lattice, the 't Hooft string tension will be smaller (or equal) to Wilson's [14] string tension. But, in the infinite volume continuum limit the various lattice definitions of the string tension are supposed to agree. A thorough investigation of inequalities between different string tensions has been carried out by Borgs and Seiler [15].

Here, we consider 't Hooft's string tension. Due to the N^3-fold toron degeneracy, it is zero to all orders of the perturbative small volume expansion. The degeneracy is lifted by tunneling between the toron sectors. A semiclassical approximation has recently been calculated by van Baal and Koller [16]. Tunneling is signaled by a rapid increase of $\sqrt{K}/m(0^{++})$, where the perturbative results [5,17] are taken for $m(0^{++})$. As soon as tunneling sets on, the validity of the present semiclassical approximation breaks down. Therefore, no quantitative results for $\sqrt{K}/m(0^{++})$ are obtained for z_0 beyond the tunneling region. For such (larger) z_0-values one has still to rely on numerical simulations. The relevant achievement of the semiclassical calculation is an analytic estimate for the z_0-value, z_0^t, where tunneling becomes relevant. The precise value of z_0^t depends somewhat on its accurate definition and on the detailed way, the semiclassical results are handled [2]. Crude estimates are

$$1.0 \leq z_0^t \leq 1.4 \text{ for } SU(2) \tag{6a}$$

and

$$z_0^t \approx 1.6 \text{ for } SU(3). \tag{6b}$$

1c) Very large z_0

For $z_0 \to \infty$ the continuum box approaches its infinite volume limit. In case of the spectrum, this approach is quantitatively controled by the equation

$$M(\infty) - M(z_0) < M(z_0)\, c_0\, \exp(-\frac{\sqrt{3}}{2} z_0) + \text{higher orders},\ c_0 > 0. \tag{7}$$

Using arguments valid to all orders of perturbation theory, equation (7) has been derived by Lüscher [18]. The constant c_0 may be related to the three glueball coupling constant. Once the range of validity of equation (7) is reached, the exponentially small corrections are very restrictive. The infinite volume approach of the 't Hooft string tension is much slower, because possibly large power law corrections are involved:

$$K(\infty) - K(z_k) = K(z_k)\, (\frac{c_k}{z_k^2} + O(\frac{1}{z_k^4})). \tag{8a}$$

Involving string theory [19] and other heuristic arguments [20] a good guess is

$$c_k = \frac{\pi}{3}. \tag{8b}$$

2) MONTE CARLO SIMULATIONS

Masses as well as the string tensions are related to eigenvalues of the transfer matrix. In the case of the standard Wilson action the transfer matrix is positive definite [21] and our forthcoming discussion is for this case. The standard method to extract eigenvalues of the transfer matrix is to consider correlation functions, $\rho(t_z)$, between **local zero-momentum trial operators**; see Ref.[22,23] for details concerning the mass-spectrum. Within the standard method the art is to find good trial operators. For sufficiently large β-values Polyakov loops $P(t_z)$ work well. In the fundamental representation they are creation operators for the 't Hooft electric flux and give rise to the 't Hooft string tension via

$$\rho_F(t_z) = < P_F(0)P_F(t_z) > \sim \exp(-E(L)t_z),\ t_z \to \infty \qquad (9a)$$

and

$$KL = E(L); \qquad (9b)$$

see section 1b) above. Polyakov loops in the adjoint representation carry zero electric flux and may be used as trial operators for glueballs [6]. Eigenstates of the transfer matrix form a complete set of operators and

$$\rho_A(t_z) = < P_A^R(0)P_A^R(t_z) >_c = \sum_n |a_n|^2 \exp(-m_n t_z) \sim \exp(-m_1 t_z),\ t_z \to \infty \qquad (10)$$

holds, where $R = A_1^{++}, E^{++}, ...$ denotes a representation of the cubic group and m_1 is the mass gap for this representation. Effective masses, $m(t_z)$, are defined by making a "cosh" fit to correlations at distance t_z and $t_z - 1$,

$$\frac{\rho_A(t_z)}{\rho_A(t_z-1)} = \frac{\exp[-m(t_z)t_z] + \exp[-m(t_z)(L_z - t_z)]}{\exp(-m(t_z)(t_z-1)] + \exp[-m(t_z)(L_z - t_z + 1)]}. \qquad (11)$$

Similarly, effective string tensions $K(t_z)$ and corresponding square roots $\sqrt{K(t_z)}$ are obtained from equation (9). Whatever these effective masses are, it is important to note that they are **upper bounds** on the mass gap in the considered channel and, if the trial operator couples to the mass gap, we have $m_1 = lim_{t_z \to \infty} m(t_z)$ ($L_z \to \infty$ first). Consequently, reliable low effective masses are in any case interesting results. My discussion of equation (11) neglects possibly important box temperature (5) effects, to be discussed elsewhere [2]. Here, I only like to emphasize that box temperature may lead to **too low** effective masses.

For β sufficiently large the short distance behaviour for adjoint Polyakov loops is $\sim t_z^{-1}$, whereas it is $\sim t_z^{-5}$ in case of the plaquette operator. This simple dimensional observation is presumably the key for understanding why adjoint Polyakov loops are good and Wilson loops are bad trial operators at large β-values. On the other hand, the signal from adjoint Polyakov loops dies rapidly away for too low $\beta = \beta(L)$-values. At intermediate β-values DLR [12] improved measurements are crucial to gain a signal from Polyakov loops.

2a) Monte Carlo Data

The improvement of numerical results can only be judged by having a look at the quality of the produced data. In case of glueballs a scale is set by previous MC variational calculations [23]. For the $A1^+$ (0^+) state Table 1 collects high statistics $SU(2)$ data from $4^3 16$-[24] and $8^3 8$-lattices [25]. The typical statistics in sweeps per data point is ≥ 30000 sweeps for the first [24] and 60000 sweeps for the second [25] case. In the second case the effective masses are the "best" (=lowest at distance $t_z = 1$) values obtained from correlations out of a list of 28 Wilson loop trial operators. Error bars are given in parenthesis and apply always to the last digits of the corresponding data point. No reliable results exist for $t_z \geq 4$. The interpretation of the data is as follows: For sufficiently low β-values ($\beta \leq 2.24$ for the $4^3 16$-lattice and $\beta \leq 2.40$ for the $8^3 8$-lattice) the optimistic hope is that the upper bounds, obtained at distance $t_z = 2, 3$, are already good approximations for the asymptotic value m_1. For larger β-values such a claim is manifestly wrong: On a finite lattice, the true mass gap is known to be a decreasing function of β. In contrast, the effective masses of Table 1 increase on the $4^3 16$-lattice for $\beta > 2.25$. This means, they become (very) poor upper bounds. The same qualitative behaviour is found on the $8^3 8$-lattice for $\beta > 2.4$ (the set of considered operators is larger in that case). An explanation is provided by spin wave calculations for short distance correlations between one-plaquette operators, see Ref.[22,24,26].

Table 1

Icosahedral subgroup, effective $m(0^+)$ masses from Ref.[24] ($4^3 16$-lattice) and Ref.[25] ($8^3 8$-lattice).

β	$L^3 L_z$	$m(1)$	$m(2)$	$m(3)$
2.0000	$4^3 16$	2.28 (2)	2.20 (10)	noise
2.0650	$4^3 16$	2.03 (2)	1.72 (05)	noise
2.1250	$4^3 16$	1.83 (2)	1.71 (08)	noise
2.1875	$4^3 16$	1.69 (2)	1.42 (05)	1.12 (10)
2.2500	$4^3 16$	1.67 (2)	1.27 (03)	1.06 (14)
2.3000	$4^3 16$	1.76 (1)	1.32 (04)	1.24 (08)
2.3750	$4^3 16$	1.96 (2)	1.57 (11)	1.6 (large)
2.2000	8^3 8	1.78 (3)	1.68 (14)	2.0 (large)
2.2500	8^3 8	1.68 (2)	1.40 (08)	1.14 (23)
2.3500	8^3 8	1.72 (3)	1.36 (09)	1.04 (31)
2.4000	8^3 8	1.78 (3)	1.11 (09)	0.83 (21)
2.5000	8^3 8	2.03 (3)	1.25 (11)	0.80 (23)

With Wilson loop trial operators the signals for the $A1^+$ state are the best among all the considered representations of the cubic group. The second best signals are found for the E^+ (2^+) state, but the correlations are already too noisy to give any restrictive $m(2^+)$-estimates. The results of Table 1 should be compared with the effective mass values of Tables 2, relying on adjoint Polyakov loops. For the moment, let us only consider data with an accuracy better or equal to 5% . Table 2a collects data from runs with the icosahedral subgroup at $\beta = 2.7$ on an $4^3 64$-lattice. From our discussion of Table 1 it is clear, that with these parameters Wilson loop trial operators would give completely irrelevant upper bounds for m_1. This is not the case with adjoint Polyakov loops. Let us call effective masses "consistent" when their error bars overlap. For $m(0^+)$ consistent effective masses $m(t_z)$ are found in the range $4 \leq t_z \leq 6$. Effective masses at distance t_z and $t_z + 1$ are, of course, not independent but highly correlated MC data. Therefore, it is not clear whether the systematic lowering for increasing t_z is a real feature or a statistical fluctuation. For large t_z error bars may become unreliable due to very large relaxation times for the large distance correlations. An optimistic estimate for the asymptotic mass, m_1, would be 0.64 ± 0.02, whereas a more conservative attitude would give 0.62 ± 0.04. It is a general shortcoming of nowadays spectroscopic analysis of MC generated correlation functions, that a subjective factor is always involved in asymptotic mass estimates. It would be highly desirable, to eliminate this subjective judgement in favour of a purely statistical approach, based on first principles about the known general behaviour of positive definite correlation functions. Unfortunately, such an approach is not straightforward, although not hopeless in the opinion of the author. However, at the moment we are plagued by rather subjective elements in the data analysis. This remark also applies to the various fit procedures that can be found in the literature. Normally a fit procedure better hides extrapolation problems than the analysis of effective masses, used here, does. In any case it is obvious that the standards of analysis allowed by Table 2a are definitely favourable as compared to those of Table 1.

The 2^+ data of Table 2a are even better than those for 0^+. Consistent effective masses are found in the range $4 \leq t_z \leq 7$ and $m(3)$ is only slightly higher, indicating a rather fast approach to the asymptotic value m_1. The $t_z = 5$ result 0.528 ± 0.010 seems to be a good asymptotic estimate. Again, we tentatively interpret the lowering at larger distances as a statistical fluctuation. Finally, the string tension data are the best, i.e. the effective $\sqrt{K}(t_z)$-estimates are very stable in t_z. According to all standards of the field the asymptotic behaviour is established. Within our rather restrictive 5% accuracy cut, consistency is found over the large range $3 \leq t_z \leq 20$. However, a more careful discussion of box temperature effects is required and will be given in Ref.[2]. For the ratios $m(0^+)/m(2^+)$ and $\sqrt{K}/m(2^+)$ we have included effective estimates with error bar estimates that take into account correlations between the masses. Normally these error bars are slightly smaller than those obtained by treating the different effective masses as uncorrelated. Due to equation (10) different effective masses have, for increasing t_z, systematic corrections with the same sign. Therefore, a better stability in t_z may be expected for mass ratios than for single masses. The stability of the $0^+/2^+$ ratio down to very small

Table 2a.

Icosahedral subgroup, effective masses for $\beta = 2.7$, $L^3 L_z = 4^3 64$, 402000 sweeps.

t_z	$m(0^+)$	$\frac{m(0^+)}{m(2^+)}$
01	1.523 (04)	1.249 (04)
02	0.740 (05)	1.281 (08)
03	0.678 (06)	1.255 (11)
04	0.659 (11)	1.238 (21)
05	0.646 (19)	1.224 (36)
06	0.619 (32)	1.173 (60)
07	0.57 (06)	1.11 (11)
08	0.57 (08)	1.19 (20)
09	0.57 (17)	1.23 (43)
10	noise	noise

t_z	$m(2^+)$	$\frac{\sqrt{K}}{m(2^+)}$
01	1.2195 (20)	0.1603 (03)
02	0.5777 (21)	0.2854 (09)
03	0.5397 (33)	0.2987 (13)
04	0.5320 (61)	0.3012 (27)
05	0.528 (10)	0.303 (05)
06	0.527 (15)	0.302 (07)
07	0.514 (24)	0.309 (13)
08	0.48 (04)	0.333 (25)
09	0.47 (06)	0.339 (40)
10	0.46 (09)	0.34 (07)
11	0.40 (12)	0.40 (12)
12	noise	noise

t_z	$\sqrt{K}$
01	0.1955 (02)
02	0.1649 (04)
03	0.1612 (06)
04	0.1602 (08)
05	0.1597 (10)
06	0.1593 (12)
07	0.1588 (15)
08	0.1586 (18)
09	0.1583 (21)
10	0.1580 (24)
11	0.1578 (28)
12	0.1575 (31)
13	0.1574 (35)
14	0.1576 (39)
15	0.1576 (44)
16	0.1577 (49)
17	0.1580 (54)
18	0.1579 (58)
19	0.1575 (61)
20	0.1576 (66)
21	0.158 (08)
22	0.158 (08)
23	0.158 (09)
24	0.159 (10)
25	0.159 (11)
26	0.159 (12)
27	0.160 (13)
28	0.160 (13)
29	0.160 (14)
30	0.161 (14)
31	0.161 (14)
32	0.163 (14)

Table 2b.

$SU(2)$ full group, effective masses for $\beta = 2.7$, $L^3 L_z = 4^3 64$, 640000 sweeps.

t_z	$m(0^+)$	$\frac{m(0^+)}{m(2^+)}$
01	1.521 (03)	1.247 (03)
02	0.745 (04)	1.281 (07)
03	0.686 (03)	1.249 (06)
04	0.673 (05)	1.227 (09)
05	0.689 (11)	1.247 (21)
06	0.739 (26)	1.318 (52)
07	0.86 (08)	1.55 (15)
08	noise	noise
	⋮	
	$m(2^+)$	$\frac{\sqrt{K}}{m(2^+)}$
01	1.2197 (13)	0.1611 (02)
02	0.5814 (11)	0.2836 (06)
03	0.5492 (16)	0.2969 (09)
04	0.5482 (27)	0.2965 (14)
05	0.5528 (42)	0.2941 (21)
06	0.560 (07)	0.2903 (37)
07	0.556 (14)	0.293 (07)
08	0.552 (27)	0.295 (15)
09	0.554 (49)	0.295 (27)
10	0.50 (09)	0.326 (51)
11	0.38 (10)	0.43 (10)
12	noise	noise

t_z	$\sqrt{K}$
01	0.1965 (02)
02	0.1649 (03)
03	0.1631 (04)
04	0.1625 (05)
05	0.1626 (06)
06	0.1627 (07)
07	0.1628 (08)
08	0.1630 (10)
09	0.1633 (11)
10	0.1638 (13)
11	0.1642 (14)
12	0.1646 (16)
13	0.1650 (19)
14	0.1654 (22)
15	0.1657 (25)
16	0.1662 (29)
17	0.1664 (32)
18	0.1664 (36)
19	0.1665 (41)
20	0.1670 (46)
21	0.1677 (52)
22	0.1685 (58)
23	0.1692 (64)
24	0.1696 (70)
25	0.170 (08)
26	0.171 (09)
27	0.171 (09)
28	0.172 (10)
29	0.174 (10)
30	0.175 (11)
31	0.177 (11)
32	0.177 (12)

Table 2c.

Icosahedral subgroup, effective masses for $\beta = 2.55$, $L^3 L_z = 8^3 32$, 322000 sweeps.

t_z	$m(0^+)$	$\frac{m(0^+)}{m(2^+)}$
01	5.52 (29)	1.018 (64)
02	1.18 (29)	1.18 (36)
03	0.678 (12)	1.165 (19)
04	0.613 (21)	1.20 (05)
05	0.549 (34)	1.09 (08)
06	0.509 (54)	1.02 (12)
07	0.48 (11)	0.99 (25)
08	0.44 (17)	0.97 (43)
09	noise	noise
	$m(2^+)$	$\frac{\sqrt{K}}{m(2^+)}$
01	5.43 (13)	0.047 (02)
02	1.00 (13)	0.149 (20)
03	0.581 (06)	0.241 (03)
04	0.510 (11)	0.269 (06)
05	0.505 (17)	0.270 (09)
06	0.498 (29)	0.273 (16)
07	0.487 (48)	0.279 (27)
08	0.454 (62)	0.299 (40)
09	0.50 (14)	0.27 (08)
10	0.51 (18)	0.27 (10)
11	noise	noise

t_z	$\sqrt{K}$
01	0.2565 (05)
02	0.1494 (05)
03	0.1400 (07)
04	0.1373 (09)
05	0.1362 (11)
06	0.1359 (14)
07	0.1358 (17)
08	0.1357 (20)
09	0.1360 (24)
10	0.1361 (28)
11	0.1361 (31)
12	0.1360 (34)
13	0.1357 (38)
14	0.1355 (41)
15	0.1363 (42)
16	0.1391 (43)

---

t_z-values should be noticed. The situation is different for $\sqrt{K}/m(2^+)$. As $\sqrt{K}$ itself is very stable in t_z, the ratio $\sqrt{K}/m(2^+)$ is spoiled by the instabilities of $m(2^+)$.

The data of Table 2b are taken with the full $SU(2)$ group. Lattice and coupling constant parameters are identical with those of Table 2a. A few values, in particular $\sqrt{K}(1)$, indicate discrepancies that might be attributed to be due to the difference between the full group and its icosahedral approximation. Otherwise, fairly consistent results are obtained for the physically interesting observables. For Table 2a we liked to interpret the lowering of effective glueball masses at large distances as a statistical fluctuation. The new

results with the full group obviously support this. Somewhat higher asymptotic estimates (0.673 ± 0.005 for 0^+ and 0.548 ± 0.003 for 2^+) are favoured.

Table 2c collects data that are closer to the region of parameter values, where the Polyakov loops fail to be good trial operators. The relevance of the DLR [12] improved measurements is clearly seen by noting that distance $t_z = 2$ results cannot be improved, whereas distance $t_z = 3$ results are improved. For the 0^+ glueball mass we cannot stay anymore within a 5% accuracy requirement, but we have to replace it by about 10% . The price paid is that the likelihood to introduce spurious data into the analysis increases. The 0^+ masses at distance $t_z = 5, 6$ are consistent, leading to an estimate 0.51 ± 0.04. Compared with the 0^+ ($\beta = 2.5$) result from Table 1 the achieved accuracy is still impressive. Again, the quality of 2^+ is even better. Consistent results in the range $4 \leq t_z \leq 7$ give 0.50 ± 0.03. The $0^+/2^+$ mass ratio is of order 1 for this data point. A 2^+ mass slightly lower than 0^+ is favoured, if one is willing to rely on the precise mass ratios from smaller distances ($t = 3, 4$) as an indicator. The highest t_z-values that have some statistical significance are 1.09 ± 0.09 ($t_z = 5$) and 1.02 ± 0.12 ($t_z = 6$).
The string tension results are still rather good. For $\sqrt{K}$ we can stay within our previous 5% accuracy cut, and the effective $\sqrt{K}(t_z)$-masses are consistent for $4 \leq t_z \leq 16$, i.e. nearly for the entire available range.

In our short discussion of data we stayed with the $SU(2)$ gauge group, because our $SU(3)$ data [2,7] are mainly exploratory and in a less convincing shape. The major reason is a notorious factor of order ten needed in computer time. For my illustration here, it seems first of all relevant to demonstrate the accuracy that may be achieved also for $SU(3)$, once sufficiently powerful computers become available. Full details for our present $SU(2)$ and $SU(3)$ data will be given elsewhere [2].

2b) Numerical $SU(2)$ Results

With an enhanced statistics, Figure 5 reproduces the $SU(2)$ $0^+/2^+$ estimates of Ref.[7]. Data from different lattices and β-values are plotted versus z_2 and they provide evidence that we are close to Fisher's universal curve. The scale of Figure 5 is choosen such that the z_2-dependence becomes clearly visible. For small z_2 contact is made with the analytic calculation by Lüscher and Münster [5] that converges up to $z_2 \approx 1.3$. A small discrepancy is seen and could be due to higher order corrections of the small volume expansion or due to tunneling. In the other limit (z large), equation (7) is valid for a sufficiently large continuous box and implies for the $0^+/2^+$ mass ratio

$$R(\infty) - R(z) \;=\; R(z)\; c_R \;\exp(-\frac{\sqrt{3}}{2}z) \;+\; \text{higher orders}, \quad \text{for } z \to \infty, \qquad (12)$$

where $z = \min(z_0, z_2)$. Assuming that this asymptotic equation is already valid in the range $2 \leq z_2 \leq 5$, we may determine the unknown constant to be $c_R \approx -1.8$. Then, the expected finite volume correction for extrapolating from $z_2 = 5$ to $z_2 = \infty$ comes out to

be $< 3\%$. This is much smaller than the statistical and subjective uncertainty of our MC calculation of the ratio at $z_2 \approx 5$. Consequently, an infinite volume limit of the order

$$R(\infty) \;=\; \frac{m(0^+)}{m(2^+)} \;=\; 1 \pm 10\% \tag{13}$$

is supported. The mean value and the error estimate are subjective in the discussed sense. A desirable and possible improvement is a better numerical control of the universal curve for $z_2 \leq 5$. Of course, the validity of the asymptotic equation (12) may be questioned altogether in this z_2-range. So far, I am not aware of any strong arguments in favour or against it. Reliable mass ratios for $z_2 > 5$ would be very interesting, but this would require some innovative progress.

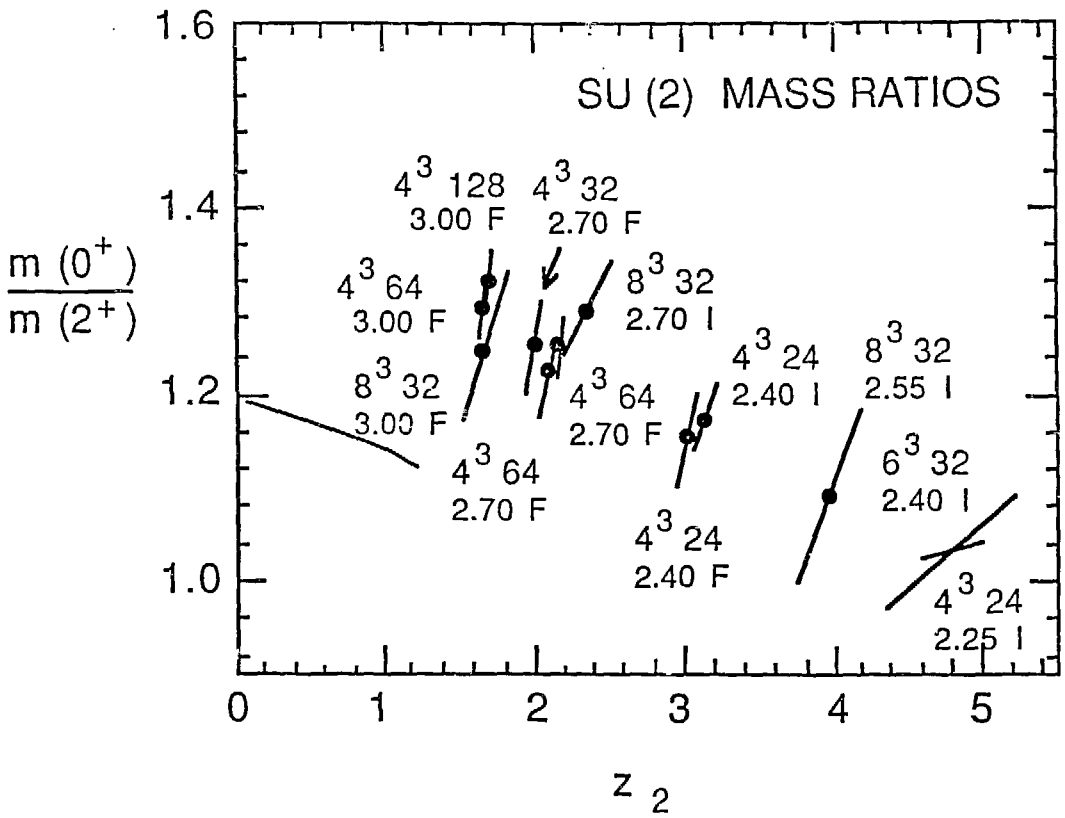

Figure 5 :

MC results for $SU(2)$ mass ratios as function of z_2. 'F' labels data taken with the full group and 'I' data taken with the icosahedral subgroup. The full line on the left is the perturbative result of Lüscher and Münster [5] (Figure 4b).

Figure 6a and 6b illustrate in more detail the z-dependence of the mass gap in units of Λ_L. Figure 6a is an updated version of an analog figure of Ref.[6] and presents 2^+ data [7] or 2^+ data with a small by-mixture of 0^+ [6]. Again, an universal curve is supported. For high β-values (2.70 and 3.00) the $8^3 32$-lattices are somewhat out of tune. Presumably this is due to too large box temperature and calculations with larger L_z-values have to be done.

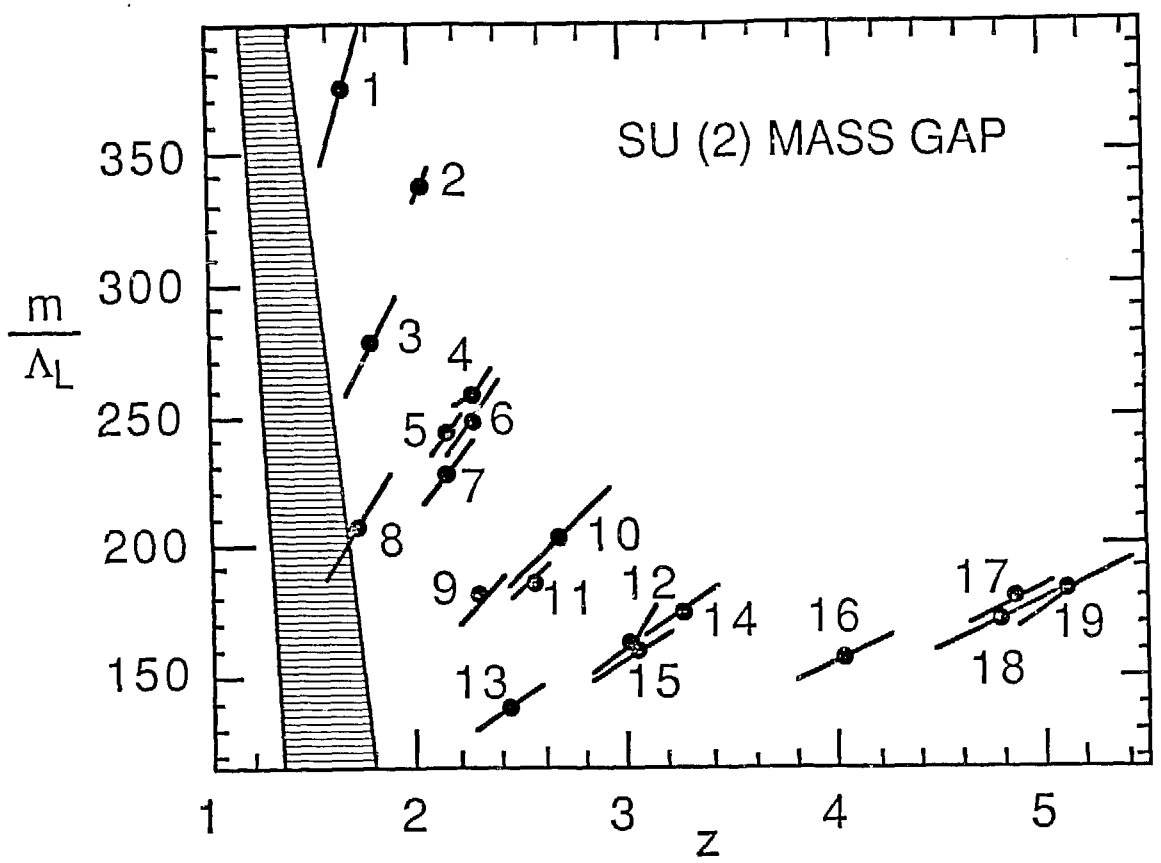

Figure 6a :

$SU(2)$ mass gap as function for z_2. The shaded region indicates the perturbative result [5] from Figure 4a. As listed in the following, the lattice sizes and β-values correspond to the labels in the figure.

$2^3 32, 2.25, (11)$	$2^3 32, 2.40, (7)$	$2^3 32, 2.55, (3)$	$2^3 60, 2.70, (1)$	
$4^3 64, 2.25, (17)$	$4^3 24, 2.40, (12)$	$4^3 24, 2.40, (14)$	$4^3 32, 2.55, (9)$	$4^3 64, 2.70, (4)$
$4^3 64, 2.70, (5)$	$4^3 64, 2.85, (2)$			
$6^3 32, 2.40, (18)$	$6^3 24, 2.40, (19)$	$6^3 32, 2.55, (15)$	$6^3 64, 2.70, (10)$	$6^3 64, 2.85, (6)$
$8^3 32, 2.55, (16)$	$8^3 32, 2.70, (13)$	$8^3 32, 3.00, (8)$		

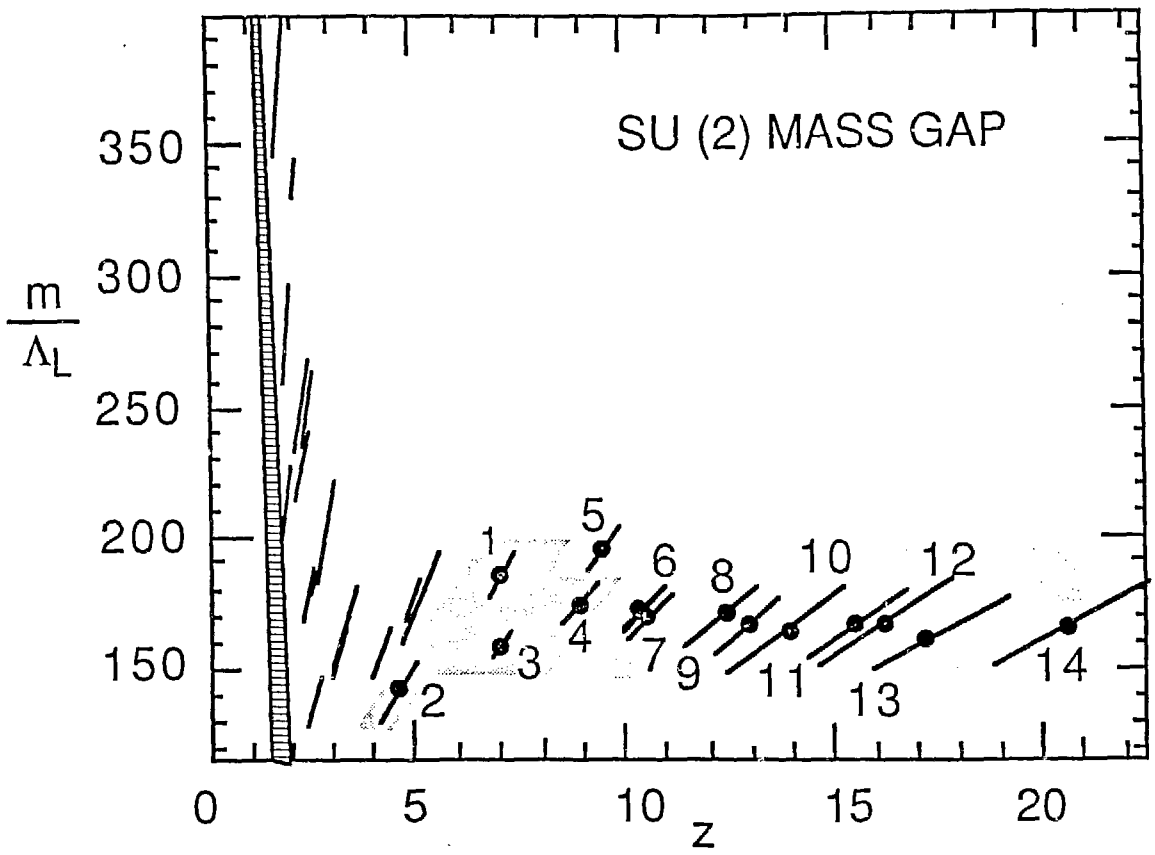

Figure 6b :

$SU(2)$ mass gap results of Figure 6a in connection with results of Ref.[24] (dark shaded region) and Ref.[27] (light shaded region). $z = \min(z_0, z_2)$. As listed in the following, the lattice sizes and β-values correspond to the labels in the figure.

$4^3 16, 2.00, (4)$	$4^3 16, 2.063, (3)$	$4^3 16, 2.125, (1)$	$4^3 16, 2.188, (2)$	Ref.[24]
$8^3 8, 2.20, (7)$	$8^3 8, 2.30, (5)$	$10^3 10, 2.20, (9)$	$10^3 10, 2.30, (6)$	Ref.[27]
$12^3 12, 2.20, (11)$	$12^3 12, 2.30, (8)$	$14^3 14, 2.20, (13)$	$14^3 14, 2.30, (10)$	Ref.[27]
$16^3 16, 2.20, (14)$	$16^3 16, 2.30, (12)$			Ref.[27]

Figure 6b depicts the same data in connection with other results [24,27]. This combination of 2^+ and 0^+ data is reasonable because of equation (13). Depending on the data point, z is z_2 or z_0. The data of Ref.[25] are not included, because they seem to be less accurate than the data by DeGrand and Peterson [27]. My overall conclusion is that

within the (rather bad) MC accuracy no finite volume corrections for $z > 5$ are visible. A shortcoming of the very large z-data [27] is that they are based on only two different β-values, what opens the possibility of an accidentally flat behaviour in z. The source method of Mütter and Schilling [28] is used in Ref.[27]. Strictly speaking the spin-parity assignment is therefore unknown. As the source method relies essentially on plaquette-plaquette correlations, a requirement of consistency with Ref.[24] implies $A1^+$ for the spin-parity assignment, and Figure 6b supports that this state has approached its asymptotic value around $z \approx 5$. The only way to spoil equation (13) would be a significantly different z-dependence of the E^+-representation for $z > 5$.

A plot of $\sqrt{K}/m(2^+)$ is less instructive than a plot of the mass ratio $m(0^+)/m(2^+)$. First, according to equations (8) we expect relevant finite volume corrections for $\sqrt{K}$ and this makes the $z \to \infty$ extrapolation more subtle than for glueballs. Second, various technical problems [2] have so far prevented us from obtaining a reliable check on the analytic tunneling prediction of equation (6a). And third, the very good numerical accuracy for $\sqrt{K}$ becomes spoiled in the ratio $\sqrt{K}/m(2^+)$ by the less good accuracy for $m(2^+)$. On the other hand, the excellent accuracy of the $\sqrt{K}$ results suggests to investigate violations of asymptotic scaling in detail. The straightforward approach is to plot $\sqrt{K}$ in unit of Λ_L versus z_k (2a). Figure 7 is the updated version of a similar plot of Ref.[6]. For small z_k data from lattices in the range $4 \leq L \leq 8$ form a smooth curve. This supports that asymptotic scaling violations are small and that the data are close to Fisher's universal scaling curve. However, for $z_k \geq 1.6$ a systematic lowering with increasing lattice size is indicated. The lattice size goes now up to $L = 12$ and results from even larger lattices may be reported in the future. These results rely on smaller β-values than the small z_k-results and a violation of asymptotic scaling may be a natural explanation for the lowering. The order of magnitude of the $z_k \to \infty$ extrapolation, $\sqrt{K} = \sqrt{K}(\infty)$, is the one of Ref.[6]. It should be remarked that Gutbrod [29] erroneously compared his large lattice result (for the Wilson string tension) with our result at $z_k \approx 0.75$, whereas his result belongs in the range $1.2 \leq z_k \leq 2.5$.

Under the assumption that corrections to Fisher scaling can be neglected, we may directly calculate the (a) lattice β-function from small volume physics. Let us emphasize that the corrections to Fisher scaling are of the same type as the corrections due to the finite block size in the standard block-spin approach [30]. We set the scale in units of $\sqrt{K}$. When Fisher scaling holds, points with $z_k = \sqrt{K}L$ =const belong to identical physics. Let us now keep L fixed and plot z_k versus β in Figure 8. From this plot we may read off $\triangle\beta$ for a change of L by a scale factor of two (similarly for a change by 1.5 etc.). A plot of the $\triangle\beta$ versus β is also given in Figure 8 and indicates values consistent with the block spin results by Patel and Gupta [31]. The accuracy achieved is similar too. However, our quantitative analysis [2] is very preliminary and not yet conclusive for higher β-values. In particular, problems are encountered that might be related to the icosahedral approximation for the full $SU(2)$ group.

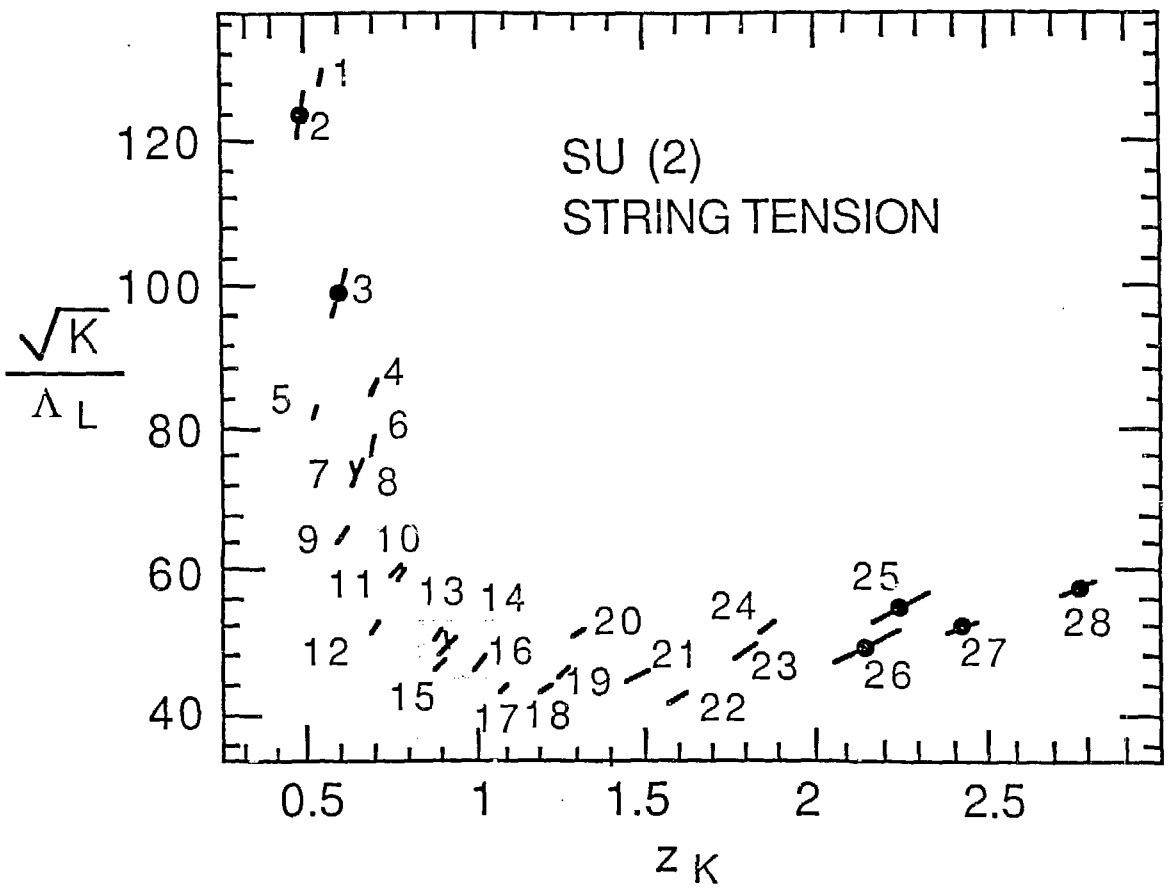

Figure 7 :

$SU(2)$ 't Hooft string tension versus z_k. The figure combines data from Ref.[2,6,7,13]. The shaded regions indicate consistent results from different lattices and β-values that support Fisher scaling. As listed in the following, the lattice sizes and β-values correspond to the labels in the figure. (Data taken with the full group are marked by 'F'.)

$2^3 32, 2.25, (12)$	$2^3 32, 2.40, (9)$	$2^3 32, 2.55, (5)$	$2^3 60, 2.75, (2)$	
$4^3 24, 2.25, (20)$	$4^3 24, 2.40, (14)$	$4^3 32, 2.55, (10)$	$4^3 64, 2.70(F), (7)$	$4^3 64, 2.70, (8)$
$4^3 64, 2.85, (3)$	$4^3 128, 3.00(F), (1)$			
$6^3 16, 2.25, (25)$	$6^3 24, 2.30, (24)$	$6^3 24, 2.40, (19)$	$6^3 32, 2.40, (18)$	$6^3 64, 2.70, (11)$
$6^3 24, 2.50, (16)$	$6^3 32, 2.55, (15)$	$6^3 64, 2.85, (6)$		
$8^3 24, 2.30, (28)$	$8^3 32, 2.40, (23)$	$8^3 32, 2.45, (21)$	$8^3 32, 2.55, (17)$	$8^3 32, 2.70, (13)$
$8^3 32, 3.00, (4)$				
$10^3 32, 2.50, (27)$	$12^3 24, 2.50, (26)$	$12^3 32, 2.55, (22)$		

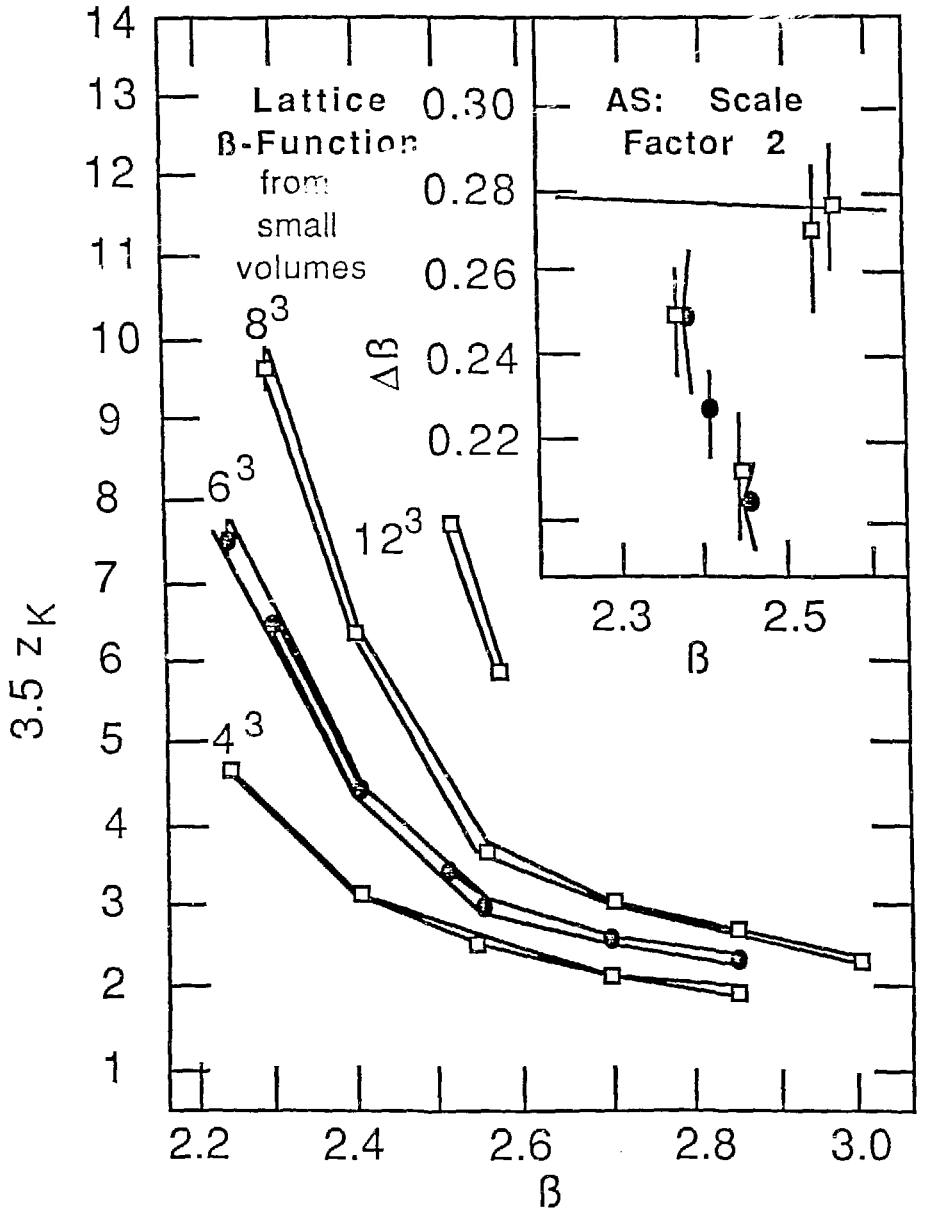

Figure 8 :

A finite size scaling analysis for the $SU(2)$ lattice β-function. The scale is set by the 't Hooft string tension. For fixed lattice size L, we plot z_k versus β and determine $\triangle\beta$ from the change of L by a factor two when we hold z_k fixed (AS = asymptotic scaling). The analysis of this figure is very preliminary.

2c) Numerical $SU(3)$ Results

Due to computer time limitations, our $SU(3)$ investigation [2,7] is essentially exploratory. Stability problems occur for increasing t_z that make the data analysis difficult and possibly unreliable. Figure 9 is an updated version of an analog figure of Ref.[7]. Relying on plausible assumptions [2], I performed a reanalysis of the data. That expains a few systematic dicrepancies (in particular for $\sqrt{K}/m(2^{++})$ at small z) between Figure 9 and Ref.[7]. The largest lattice involved is now $8^3 32$ at $\beta = 6.0$. Otherwise the results come from $4^3 L_z$- and $6^3 L_z$-lattices and there is only weak evidence that the universal scaling curve is already reached.

Let us first discuss the $m(0^{++})/m(2^{++})$ mass ratio. We disregard the high value 1.8 from the $4^3 32$-lattice at $\beta = 6.8$. It could be a statistical accident, or it may be systematically spoiled due to too small L or too small L_z. Our other data indicate values around $m(0^{++})/m(2^{++}) \approx 1.5$. The 4^3-lattices are around 1.6, but the large lattices are somewhat below 1.5. This is high, as compared with the recent $SU(3)$ small volume calculation by Weisz and Ziemann [17] that yields $m(0^{++})/m(2^{++}) \approx 1.2$. Neither the numerical nor the analytical accuracy is in a very good shape. A list of possible reasons for the discrepancy goes as follows:
1) The lattice size L may be too small and a/L-corections to Fisher scaling could, for increasing L, lead to a systematic lowering of the MC ratios.
2) For larger t_z-values, box temperature may fake effective masses that are lower than the real mass. This remark holds for the 0^{++} state as well as for the 2^{++} state. If the effect is quantitatively different for the two states, too high (or too low) mass ratios may result. We made one check with respect to L_z: At $\beta = 6.6$ ($L = 4$) we compared L_z-lattices with $L_z = 32$ and $L_z = 64$ and we did not find a notable correction for the mass ratio.
3) Higher order corrections to the small volume calculation may be large around $z_2 = 1$.
4) Tunneling may significantly change the mass ratio.
5) Everything else that you may imagine.
For larger z_2-values the mass ratio is, as for $SU(2)$, consistent with one. Again, the expected large z-corrections are less than 3%, if we are allowed to fit the constant of equation (12) with our results in the range $2 \leq z_2 \leq 5$. Of course, the MC accuracy is much less convincing as in the $SU(2)$ case. A reasonable estimate is

$$P(\infty) = \frac{m(0^{++})}{m(2^{++})} = 1 \pm 20\%. \tag{14}$$

Some heuristic arguments favour 0^{++} to be the mass gap. But, to the extent that our aim is to understand QCD from first principles, we should better be open for surprises.

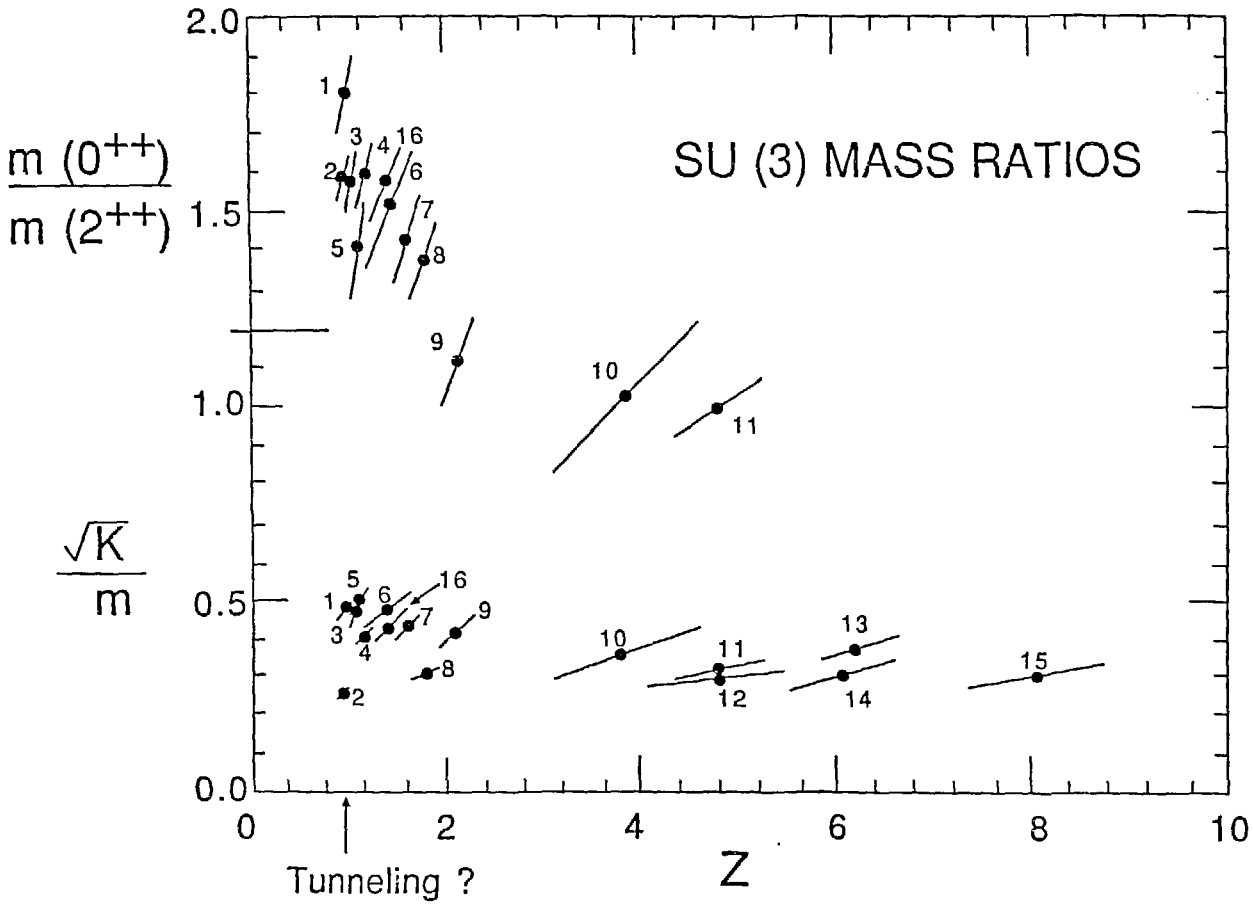

Figure 9 :

MC results for $SU(3)$ mass ratios versus $z = z_2$. The straight line around 1.2 indicates the pertubative $m(0^{++})/m(2^{++})$ results by Weisz and Ziemann [17]. In the lower part of the figure, the large z data are $\sqrt{K}/m(0^{++})$ results by De Forcrand et. al. [20,32] and by Patel et. al. [33]. In that case $z = z_0$. As listed in the following, lattice sizes and β-values correspond to labels in the figure. For low z_2 the semiclassical tunneling prediction [16] is indicated (assuming $z_0 \approx 1.5 z_2$ for $z_2 \approx 1$).

$2^3 64, 6.80, (2)$				
$4^3 32, 5.80, (9)$	$4^3 32, 6.00, (7)$	$4^3 32, 6.20, (16)$	$4^3 32, 6.40, (5)$	$4^3 32, 6.60, (4)$
$4^3 64, 6.60, (3)$	$4^3 32, 6.80, (1)$			
$6^3 32, 5.80, (11)$	$6^3 32, 6.20, (8)$	$6^3 48, 6.40, (6)$		
$8^3 32, 6.00, (10)$				
$10^3 20, 5.90, (13)$				Ref.[20,32]
$6^3 21, \quad , (12)$	$9^3 21, \quad , (14)$	$9^3 21, \quad , (15)$		Ref.[33]

The lower part of Figure 9 deals with $\sqrt{K}/m$. As in Figure 6b, we combine $m = m(2^{++})$ data for small $z = z_2$ with $m = m(0^{++})$ data for large z_0. The $\sqrt{K}/m(0^{++})$ estimates are taken from De Forcrand et. al. [20,32] and from Patel et. al. [33]. For the Wilson action, I only take data with $\beta \geq 5.8$ into account, because scaling violations are likely to appear for lower β-values. This excludes all but one ($10^3 20$, $\beta = 5.9$) data points from Ref.[20,32]. The results of Ref.[33] rely on a fundamental-adjoint mixed action and are conjectured to be rather close to the continuum limit. As Fisher's universal scaling curve does not depend on the action, it is natural to include these data. For small z_2-values only a data point from an $2^3 64$-lattice signals an onset of tunneling. Certainly we cannot expect such small L-values to be characteristic for the universal curve. To the extent that a mass ratio $m(0^{++})/m(2^{++}) \approx 1.5$ really holds close to the tunneling region, the analytic estimate (6b) would become $z_2 \approx 1.1$ with a rather large uncertainty. A quantitatively precise matching of numerical and analytical results is presently not possible. (Remark: From our comparision of an $4^3 32$ and an $4^3 64$ lattice at $\beta = 6.6$ we conclude that we previously underestimated some $m(2^{++})$, as well $m(0^{++})$, masses. On the other hand, the string tension results are found stable. This leads to corrections of some of our $\sqrt{K}/m(2^{++})$ estimates of Ref.[7]. Tentatively, these corrections [2] are now taken into account, whereas my talk was still based on uncorrected data.)

Figure 10 analyses the string tension in units of Λ_L. All data, the author is aware off [34], are collected in Figure 10a. The results is a "full house". Whereas the analog $SU(2)$ data, in Figure 6a, form a smooth curve, it does not happen for $SU(3)$. According to our general discussion, the reason could be either too small lattices or asymptotic scaling violations. The first possibility is considered by Figure 10b. Now the whole dilemma of a naive analysis of asymptotic scaling becomes obvious. The difference between the $\sqrt{K}/\Lambda_L$-values at $\beta = 5.7$ and at $\beta = 5.9$ (6.0) could be a violation of asymptotic scaling as well as a z_k-dependence. Without further data it is impossible to distinguish between the two options. In view of additional information from other investigations [35], I would like to argue in favour of asymptotic scaling violations. To investigate this, we cut-off all data with $\beta < 6.0$ and plot the remaining data in Figure 10c. The result is a remarkably smooth curve. Unfortunately, nearly no data exist for large z_k.

Figure 11a depicts the present data [2,7,32] for $m(0^{++})$ in units of Λ_L. To avoid too small masses due to box temperature, we restrict the maximum t_z, where we trust our effective masses to be upper bounds, to be $t_z = 4$ for most of the cases. Not only larger L_z, but also larger L is desirable. Presently, only one lattice has $L > 6$ and, unfortunately, the $8^3 32$, $\beta = 6.0$ $m(0^{++})$-result is fairly inconclusive. For this lattice, β is already too small to make the adjoint Polyakov loop a good trial operator. (The correlated $m(0^{++})/m(2^{++})$ mass ratio of Figure 9 is in a slightly better shape.) Because of the conjectured asymptotic scaling violation, we may like to cut-off all data with $\beta < 6.0$. Figure 11b displays the left-over data. They rely entirely on Ref.[2,7]. So far, no other method has allowed to calculate correlation functions at reasonably large distances for $\beta \geq 6.0$ on small or other lattices.

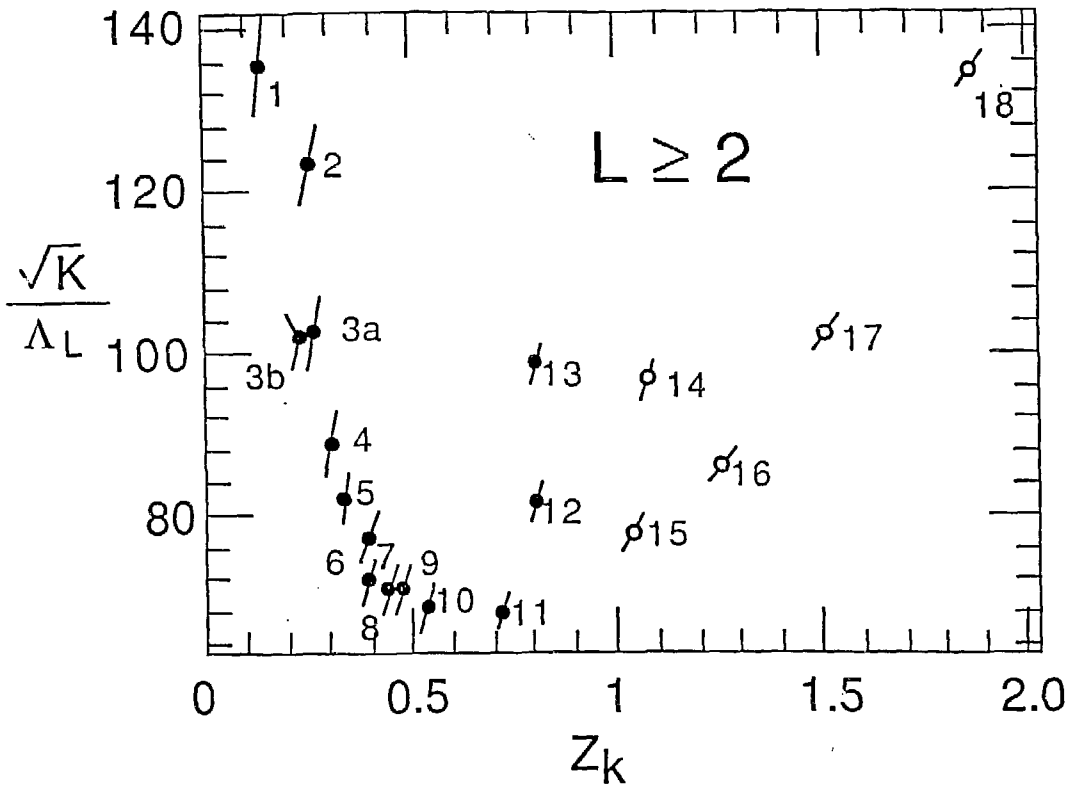

Figure 10a :

$SU(3)$ 't Hooft string tension versus z_k. The figure combines data from Ref.[2,7] (•) and Ref.[20] (○). As listed in the following, lattice sizes and β-values correspond to the labels in the figure.

$2^3 64, 6.80, (1)$				
$4^3 32, 5.60, (13)$	$4^3 32, 5.80, (9)$	$4^3 32, 6.00, (7)$	$4^3 32, 6.20, (5)$	$4^3 64, 6.40, (4)$
$4^3 32, 6.60, (3a)$	$4^3 64, 6.60, (3b)$	$4^4 32, 6.80, (2)$		
$6^3 32, 5.80, (12)$	$6^3 32, 6.00, (10)$	$6^3 32, 6.20, (8)$	$6^3 48, 6.40, (6)$	
$8^3 32, 6.00, (10)$				
$6^3 12, 5.50, (18)$	$6^3 16, 5.70, (14)$			Ref.[20]
$8^3 16, 5.70, (17)$	$10^3 20, 5.90, (16)$	$10^3 20, 6.00, (15)$		Ref.[20]

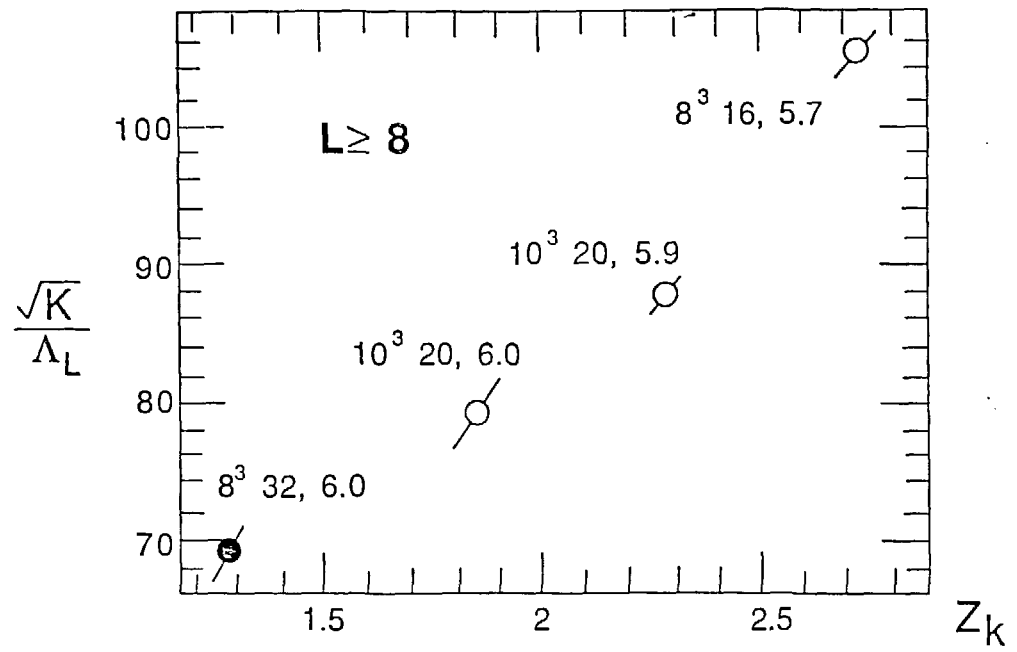

Figure 10b :

$SU(3)$ 't Hooft string tension versus z_k. Data of Figure 10a restricted to $L \geq 8$.

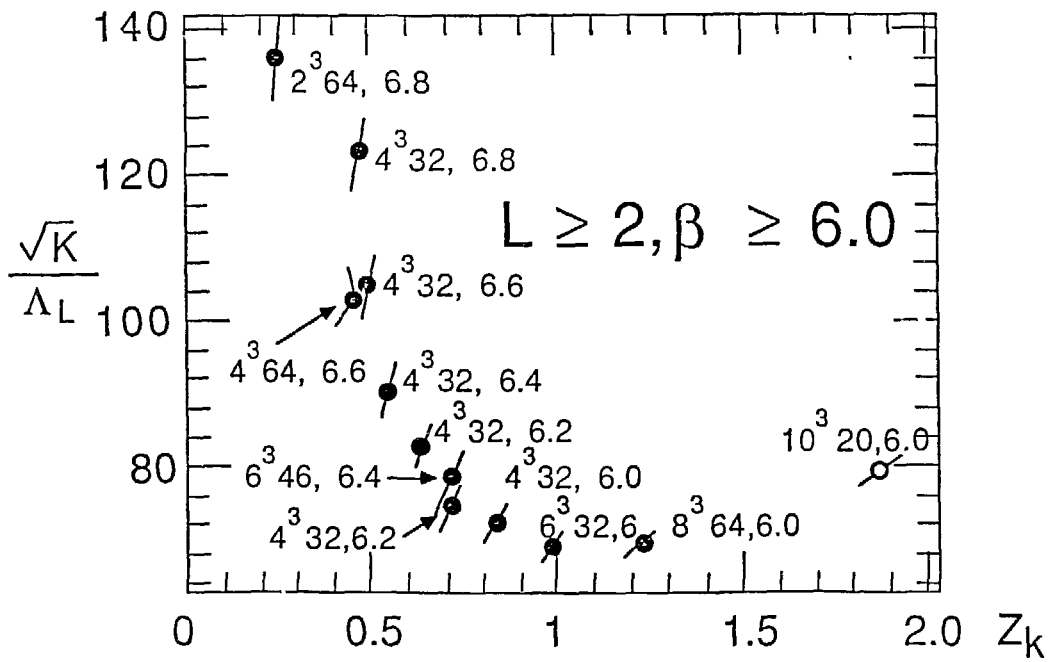

Figure 10c :

$SU(3)$ 't Hooft string tension versus z_k. Data of Figure 10a restricted to $\beta \geq 6.0$.

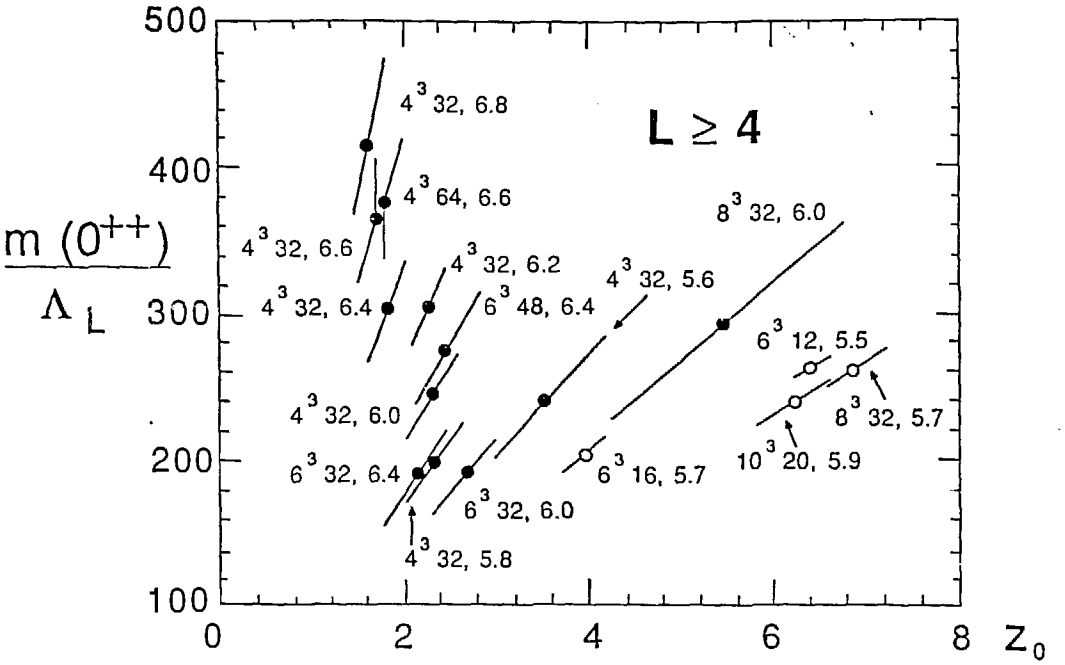

Figure 11a :

$m(0^{++})$ mass versus z_0. The figure combines data of Ref.[2,7] (•) and Ref.[32] (○).

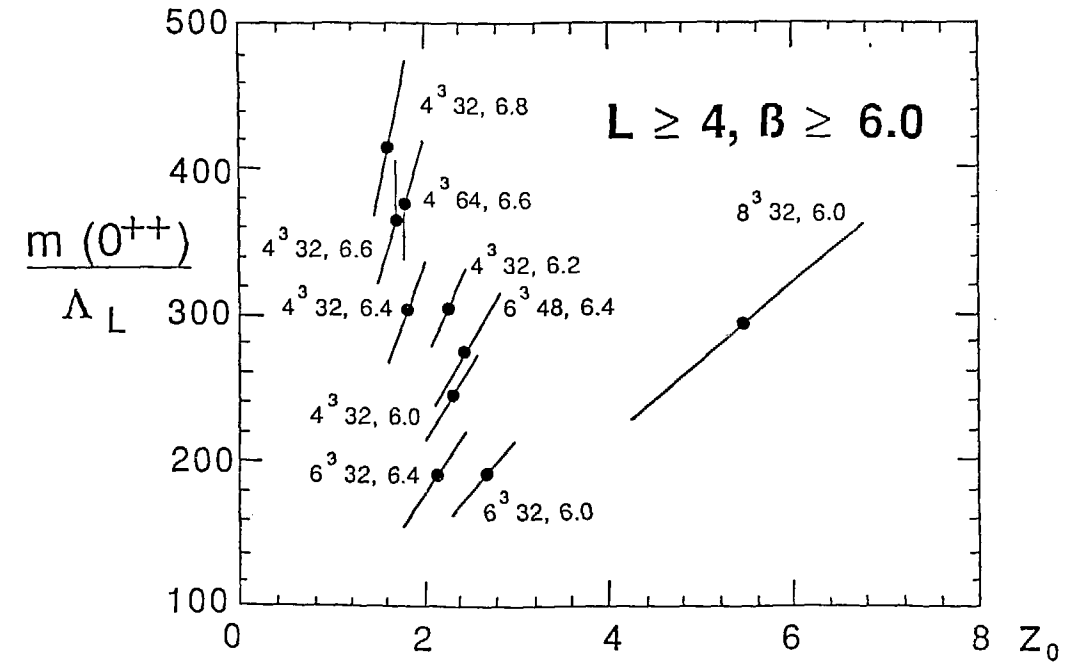

Figure 11b :

$m(0^{++})$ mass versus z_0. Data of Figure 11a restricted to $\beta \geq 6.0$.

Of course, there are no phase transitions on finite lattices. By $\mathbf{T_{ci}}$ we shall denote a signal for the critical temperature. The index $i = 1, 2, ..$ labels different signals. In the infinite volume continuum limit, $z_T \to \infty$, all signals have to give the same deconfinement temperature $\mathbf{T_c}$, but they may differ for finite systems. The $SU(3)$ standard analysis uses a signal, $\mathbf{T_{c1}}$, from scatter plots of Polyakov loop expectation values. On large lattices high statistics results were obtained by Kuti et. al.[36] and by Christ and Terrano [37]. Let us restrict ourselves to lattices with $L_t \geq 6$. In Figure 12 these results [38] are plotted

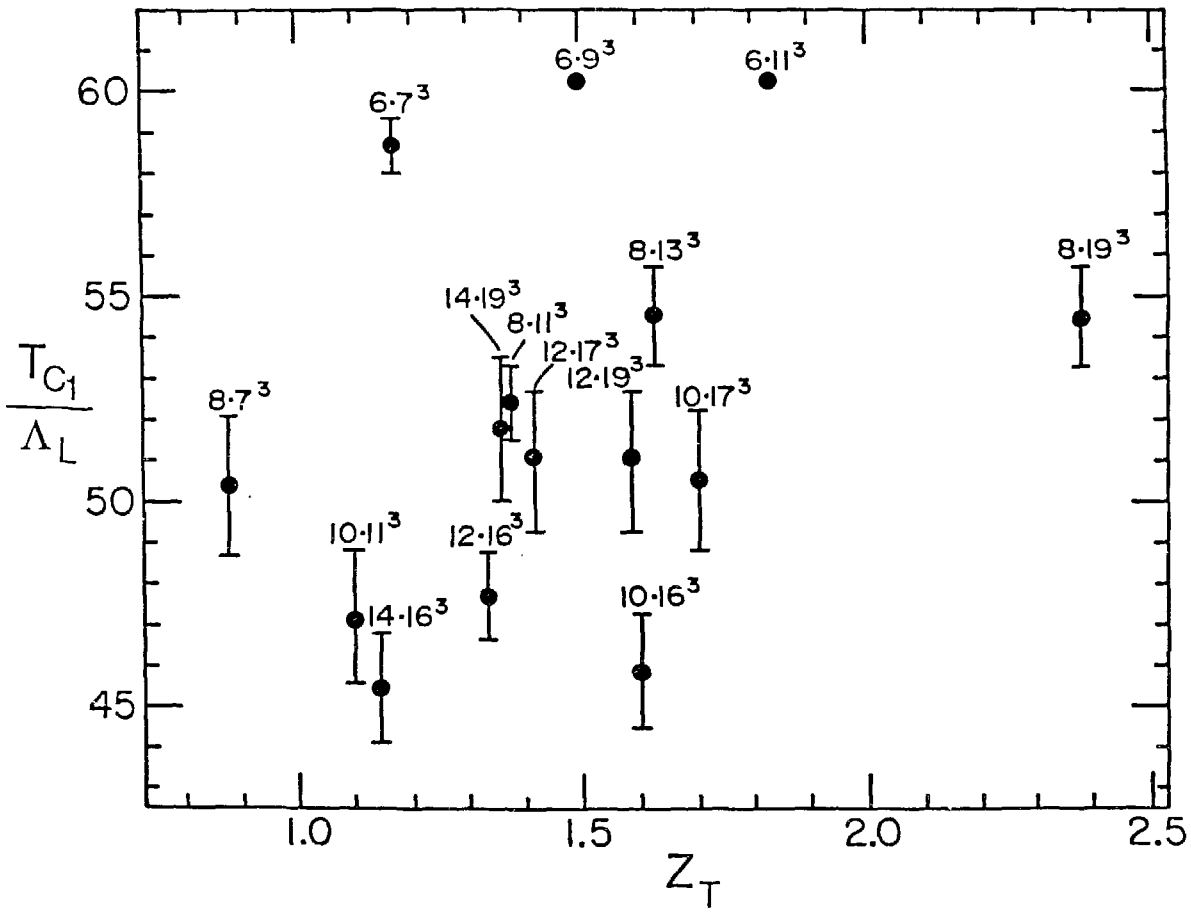

Figure 12 :

Finite size scaling plot for the T_{c1} results of Ref.[36,37]. The data are labelled by the lattice size. $L = odd$ corresponds to Ref.[36] and $L = even$ to Ref.[37].

versus the Fisher scaling variable z_T, defined by equation (2b). We study the $\beta \to \infty$ limit where T_c, like all physical masses goes to zero (second order phase transition), whereas the $SU(3)$ deconfinement phase transition is first order. The "best" results for which asymptotic scaling is claimed [36,37] have $L_t \geq 8$. If these results are relevant for the infinite volume continuum limit, $z_T \to \infty$, Figure 12 implies

$$|T_{c1}(z_T = 1) - T_{c1}(z_T = \infty)| \; = \; \text{small}. \tag{15}$$

Small means of the order of a typical error bar of the MC T_{c1}-estimates around $z_T \approx 1.4$.

Is there a relation between our MC calculations [2,6,7] on $L^3 L_z$-lattices and the calculations of Ref.[36,37] This question has been addressed in Ref.[39] and the answer is "yes". Let us consider lattices of shape

$$L_t L^2 L_z \text{ with } L_t \leq L \leq L_z. \tag{16}$$

We fix L_t and L and take $L_z \to \infty$. This does not change the transfer matrix in the z-direction. Eigenvalues of the transfer matrix determine the physics of the lattice system. With too small L_z, box temperature (5) problems may prohibite an accurate MC determination of these eigenvalues, even if the corresponding correlation functions are out of the statistical noise. L_z should be as large as possible to calculate numerically the eigenvalues of the transfer matrix, that is also the transfer matrix belonging to the $L_t L^3$-lattice. Long range correlations between Polyakov loops in the fundamental representations are required for the deconfinement phase transition, and an appropriate signal for the critical temperature, called $\mathbf{T_{c2}}$ henceforth, is the tunneling transition of the 't Hooft string tension. As for T_{c1}, the physical deconfinement temperature is reached in the infinite volume limit: $T_c = lim_{z_T \to \infty} T_{c1}(z_T) = lim_{z_T \to \infty} T_{c2}(z_T)$.

An advantage of the tunneling signal T_{c2} is that it has a direct physical interpretation for finite systems. The concept may be illustrated [2] with help of the two- and three-dimensional Ising models. Particularly nice are exact results from the two-dimensional Ising model. For $L\infty$-lattices, the tunneling transition is depicted in Figure 13a, and Figure 13b demonstrates how the maximum of the second derivative of the mass gap with respect to $g = \beta^{-1}$ is approaching the critical point β_c. (A quantitatively more usefull approach will be discussed elsewhere [2].) Qualitatively the same behaviour is found by an numerical investigation [2] of the three dimensional Ising model on $L^2 L_z$, (L_z large) lattices. This model is believed to exhibit the same critical behaviour as the $SU(2)$ deconfinement phase transition.

For $SU(N)$ lattice gauge theory, the analytic calculation by Koller and van Baal [16] and our MC calculations [2,6,7] provide information about the deconfinement signal T_{c2} at $z_t = 1$. In view of equation (15), deduced from Figure 12, we may expect

$$T_{c2}(z_T = 1) \; \approx \; T_{c1}(z_T = 1) \; \approx \; T_c. \tag{17}$$

To get an idea about the order of magnitude for $T_{c2}(z_T = 1)$, indicated by the analytic results, we may convert equations (6) into estimates of $T_{c2}(z_T = 1)$ by using the perturbative $SU(2)$ [5] and $SU(3)$ [17] spectrum calculations. Of course, this procedure can only

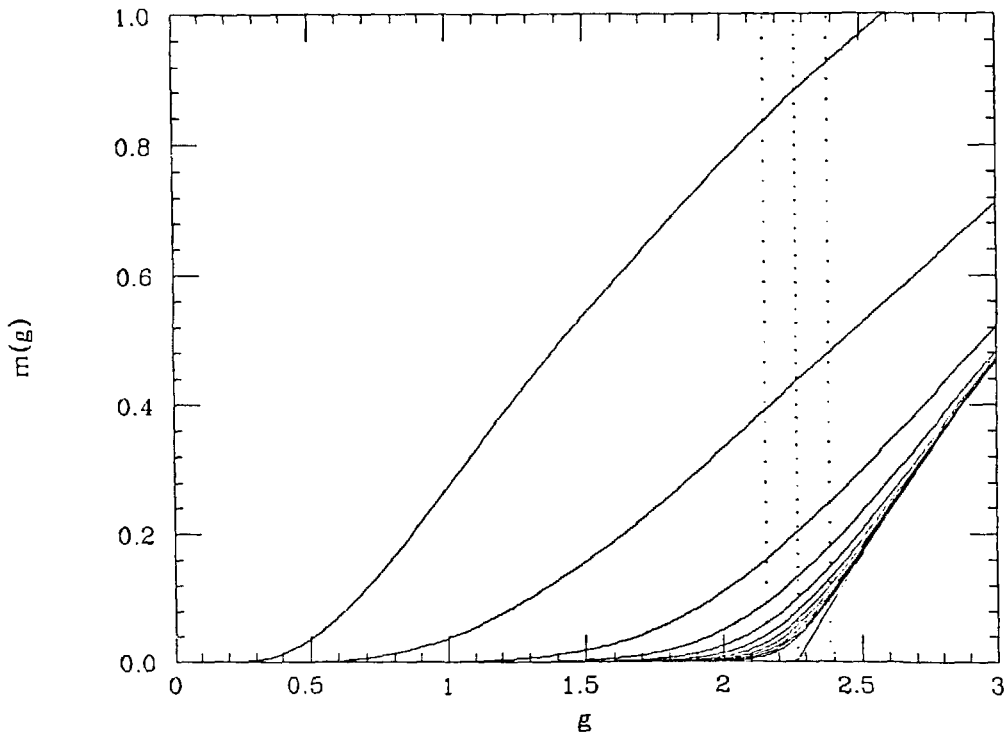

Figure 13a :

Mass gap $m(g)$ versus $g = \beta^{-1}$ for the two dimensional Ising model on $L\infty$ lattices. From left to right the curves correspond to $L = 1, 2, 4, 6, 8, ..., 16, 18, 20$. In all cases $m(g)$ is exponentially surpressed for $g \to 0$, $m(g) \sim \exp(-2/g)$ in case of the one dimensional Ising model, and similar for $L = 2, 4$, etc. . For increasing L the tunneling transition approaches the infinite volume critical temperature, as more explicitely demonstrated in Figure 13b. The three vertical lines indicate β_c and $\beta_c \pm 5\%$.

give rather crude estimates [2]. These are

$$150\Lambda_L \leq T_{c2}(z_T = 1) \leq 10^{24}\Lambda_L \text{ for } SU(2) \tag{18a}$$

and

$$T_{c2}(z_T = 1) \approx 400\Lambda_L \text{ for } SU(3). \tag{18b}$$

In principle, MC calculations allow accurater results. Presently, however, only the following [2,39] lower bounds exist:

$$125\Lambda_L \;<\; T_{c2}(z_T = 1),\; L = 8 \text{ for } SU(2) \tag{19a}$$

and

$$112\Lambda_L \;<\; T_{c2}(z_T = 1),\; L = 6 \text{ for } SU(3). \tag{19b}$$

Therefore, the first part of equation (17) is wrong and the discrepancy between T_{c1} and T_{c2} is huge for $z_T = 1$ (see Ref.[41] for $SU(2)$ T_{c1} estimates). Certainly, it is an abuse of language to speak about "phase transition" for finite lattices, when equivalent signals are still far apart from one another. The relevant question is now how the infinite volume limit $z_T \to \infty$ is approached quantitatively. Will T_{c1}, T_{c2} or both strongly depend on z_T for $z_T \to \infty$? $SU(2)$ MC simulations with $L_t < L \ll L_z$ are in progress [2].

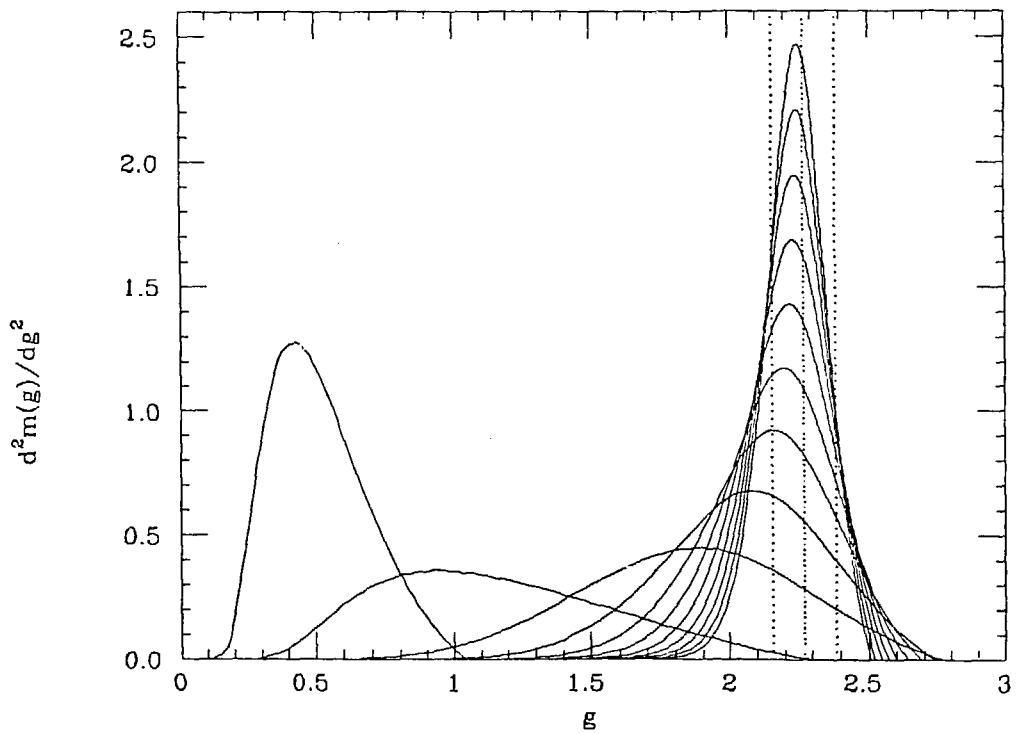

Figure 13b :

Tunneling signal for the two dimensional Ising model on $L\infty$ lattices. With increasing L, the maximum of the second derivative $\frac{d^2}{dg^2}m(g)$ is approaching the infinite volume critical temperature. (Although instructive, this is not a recommendable approach for a quantitative numerical analysis.)

4) CONCLUSIONS

Within nowadays MC investigations, the finite volume cannot be ignored. The infinite volume approach of the deconfinement temperature, in particular for the tunneling signal, is somewhat obscure and a more detailed study is in progress [2]. Our optimistic opinion [39] is that the small volume (large lattice!) $SU(3)$ results of Ref.[36,37] and the $SU(2)$ results of Ref.[41] are already close to the infinite volume limit.
For glueball masses and (to some extent) for the 't Hooft string tension we know how to control the infinite volume continuum limit. The asymptotic equation (7) for glueball masses is very restrictive, but numerical data are not yet in a completely satisfactory shape. For the 't Hooft string tension the situation is nearly the other way round. At least some numerical data exhibit an excellent quality, but the asymptotic extrapolation (8) is tedious.
Needless to say, QCD may be rather distinct from pure gauge theories due to quark interactions.

NOTE ADDED

First $SU(2)$ data [2] from $4 \cdot 4^2 64$ and $4 \cdot 6^2 64$ lattices show that, by increasing z_T from $z_T = 1.0$ to $z_T = 1.5$, the tunneling transition moves very rapidly towards the standard estimate [41] of the $SU(2)$ deconfinement temperature for an $4 \cdot L^3$, (L "large") lattice. The new MC results confirm the analysis of Ref.[39] that connects the tunneling transition with deconfinement. In the analogy of Figure 13b, the $SU(2)$ tunneling signal for an $4 \cdot 4^2 64$-lattice is similarly far apart from the deconfinement temperature, as the tunneling signal for an 2∞ two dimensional Ising model is far apart from the critical coupling $\beta = \beta_c$ of the infinite volume system.

ACKNOWLEDGEMENTS

This lecture would have been impossible without continuous collaboration with Alain Billoire. Our $SU(3)$ results rely on work with Claus Vohwinkel [2,7,39] and part of our $SU(2)$ data were obtained in collaboration with Enzo Marinari [2,13]. Further, I would like to thank Gyan Bhanot, Khalil Bitar, Dennis Duke, Anna and Peter Hasenfratz, Tony Kennedy, Roman Salvador and Peter Weisz for usefull discussions, help or correspondence. This work received support by the Department of Energy under cooperative agreement number DE-FC05-85ER25000 and from the Florida State University through use of its Cyber 205.

REFERENCES

1) M.E. Fisher, in *Critical Phenomena*, Proceedings of the 51^{th} Enrico Fermi Summer School, Varena, ed. M.S. Green (Academic Press, NY, 1972)
2) Work in preparation
3) I would like to thank M. Fisher for a usefull discussion concerning this point. The present reader is assumed to be familiar with the difference between scaling and asymptotic scaling.
4) G. 't Hooft, Nucl. Phys. B153 (1979) 141
5) M. Lüscher, Nucl. Phys. B219 (1983) 233; M. Lüscher and G. Münster, Nucl. Phys. B232 (1984) 445
6) B. Berg and A. Billoire, Phys. Lett. 166B (1986) 203 and erratum (to be published)
7) B. Berg, A. Billoire and C. Vohwinkel, Phys. Rev. Lett. 57 (1986) 400
8) A. Gonzales-Arroyo, J. Jurkiewicz and C.P. Korthals-Altes, NATO Advanced Study Institute Series, B82 (1982) 339
9) M. Lüscher, Phys. Lett. 118B (1982) 391
10) I. Bender, B. Berg and W. Wetzel, Nucl. Phys. B269 (1986) 38
11) A.M. Polyakov, Phys. Lett. 72B (1978) 477; L. Susskind, Phys. Rev. D20 (1979) 2610
12) G. Parisi, R. Petronzio and F. Rapuano, Phys. Lett. 128B (1983) 418
13) A. Billoire and E. Marinari, Phys. Lett. 139B (1984) 399
14) K. Wilson, Phys. Rev. D10 (1974) 2445
15) C. Borgs and E. Seiler, Commun. Math. Phys. 91 (1983) 329
16) J. Koller and P. van Baal, Nucl. Phys. B273 (1986) 387; P. van Baal and J. Koller, Preprint, ITB-SB-86-76
17) P. Weisz and V. Ziemann, Preprint, DESY 86-109
18) M. Lüscher, Cargèse lectures 1983, Eds. G. 't Hooft et. al., Plenum, New York (1984); Preprint, DESY, 85-144, to appear in Commun. Math. Phys.
19) M. Lüscher, K. Symanzik and P. Weisz, Nucl. Phys. B173 (1980) 365
20) Ph. De Forcrand, G. Schierholz, H. Schneider and M. Teper, Phys. Lett. 160B (1985) 137
21) M. Creutz, Phys. Rev. D15 (1977) 1128; M. Lüscher, Commun. Math. Phys. 54 (1977) 283; K. Osterwalder and E. Seiler, Ann. Phys. (N.Y.) 110 (1978) 440
22) B. Berg and A. Billoire, Nucl. Phys. B221 (1983) 109
23) B. Berg, Cargèse lectures 1983, Eds. G. 't Hooft et. al., Plenum, New York (1984)
24) B. Berg, A. Billoire and C. Rebi, Ann. Phys. (N.Y.) 142 (1982) 185 and Addendum 146 (1983) 470
25) B. Berg, A. Billoire, S. Meyer and C. Panagiotakopoulos, Commun. Math. Phys. 97 (1985) 31
26) A. Coste, A. Gonzales-Arroyo, C.P. Korthals Altes, B. Söderberg and A. Tarancon, Preprint, CPT-86/P.1876 (January 1986), (Nucl. Phys. B, to appear)
27) T.A. DeGrand and C. Peterson, Preprint, COLO-HEP-117 (June 86)
28) K. Mütter and K. Schilling, Phys. Lett. 117B (1982) 75

29) F. Gutbrod, Preprint, DESY 86-65 (June 86)
30) K. Wilson, Cargèse lectures 1979, Eds. G. 't Hooft et. al., Plenum, New York (1980), and references given there
31) A. Patel and R. Gupta, Nucl. Phys. B251 [FS13] (1985) 789
32) Ph. De Forcrand, G. Schierholz, H. Schneider and M. Teper, Phys. Lett. 152B (1985) 107
33) A. Patel, R. Gupta, G. Guralnik, G. Kilcup and S. Sharpe, Phys. Rev. Lett. 57 (1986) 1288
34) The data of Ref.[33] cannot be included, as Λ_L seems to be unknown presently.
35) For a review see A. Hasenfratz and P. Hasenfratz, Ann. Rev. Nucl. Part. Sci. 35 (1985) 559
36) A.D. Kennedy, J. Kuti, S. Meyer and B.J. Pendleton, Phys. Rev. Lett. 54 (1985) 87; S.A. Gottlieb, J. Kuti, D. Toussaint, A.D. Kennedy, S. Meyer, B.J. Pendleton and R.L. Sugar, Phys. Rev. Lett. 55 (1985) 1958
37) N.H. Christ and A.E. Terrano, Phys., Rev. Lett. 56 (1986) 111
38) Small improvements of the results of Ref.[36,37] were reported at this conference. They are not included in the present analysis.
39) B. Berg, A. Billoire and C. Vohwinkel, Preprint, FSU-SCRI-86-70
40) Some of the results of this section were added after the Brookhaven conference.
41) J. Engels, J. Jersák, K. Kanaya, E. Laerman, C.B. Lang, T. Neuhaus and H. Satz, Preprint, FSU-SCRI-86-59; G. Curci and R. Tripiccione, Phys. Lett. 151B (1985) 145